Collaborative Project
Small-medium-scale focused research project (STREP)

Grant Agreement n. 224168 FP7-ICT-2007-2

WIDE

Decentralized and Wireless Control of Large-Scale Systems

Starting date: 01 September 2008 Duration: 3 years

Deliverable number	**D3.1**
Title	**Methodologies for identification and model management of large-scale systems**
Work package	WP3 - Multilayer distributed control and model management
Due date	M22
Actual submission date	09/11/2010
Lead contractor for this deliverable	KTH
Authors	Håkan Hjalmarsson <hakan.hjalmarsson@ee.kth.se> Pavel Trnka <pavel.trnka@honeywell.com> Henrik Sandberg <henrik.sandberg@ee.kth.se> Cristian R. Rojas <cristian.rojas@ee.kth.se> Christian Larsson <christian.larsson@ee.kth.se>
Revision	v1.0 (November 9, 2010)

Dissemination Level

→	**PU**	Public
	PP	Restricted to other programme participants (including the Commission Services)
	RE	Restricted to a group specified by the consortium (including the Commission Services)
	CO	Confidential, only for members of the consortium (including the Commission Services)

Executive summary

This report summarizes results achieved in Task 3.1 of WIDE.

Contents

Background

Task 3.1 in WIDE concerns development of techniques for building models of different levels of abstraction for hierarchical control including system identification, input excitation design, the uncertainty representation and interlayer propagation and built-in model management and maintenance for consistency with structural changes in the system: system identification in the distributed, large-scale, networked environment. It also includes model management of large-scale systems with uncertainty propagation.

Two partners, Honeywell and KTH, have contributed to the task where KTH has contributed to system identification in a distributed, large-scale, networked environment whereas Honeywell has contributed to model management of large-scale systems with uncertainty propagation. Honeywell has contributed with 22MM and KTH with 10 MM to this deliverable.

Common to WP3 is that number of articles accepted for publication in peer-reviewed journals, organization of invited sessions, and possible filed patent applications are measures of success. Particular measures of success to Task 3.1 are a documented set of model management techniques demonstrated in MATLAB/Simulink, featuring (i) model ID capabilities of large-scale systems, including generation of submodels consistent with measured data; (ii) managing large-scale interconnected models with built-in complexity reduction and uncertainty propagation, ensuring cross-layer and interlayer compatibility, and able to responsively capture structural changes in the process.

1 Results summary

Deliverable D3.1 targets methodologies for identification and model management of large-scale systems. The results achieved in this deliverable are used across all work packages of WIDE project. According to work-plan coordinated between KTH and HPL, the results were achieved in the following subtasks:

3.1.1. Consistent modeling and self-maintaining models

3.1.2. Input signal design

3.1.3. System ID for large-scale systems

3.1.4. Fault-detection

The first subtask, T3.1.1, concerns consistent modeling and model management that addresses two topics: first, merging models of different quality and second, structure-respecting identification and order reduction. Regarding the former topic, HPL developed a novel methodology for merging several models of different quality for the same system considering FIR and/or ARX models. The proposed approach uses merging models in the time domain, using the concept of equivalent data. This result was published in [HPL2]. Addressing the second topic, HPL invested a significant effort to develop a new methodology for consistent combination of arbitrarily interconnected submodels with uncertainty into a complex, large-scale model. The interconnected models are assumed to be FIR and/or ARX models with parameters given by the mean and variance. The main result is obtaining a global ARX/FIR with statistically correct mean and variance. This result was also published in [HPL2]. Another novel solution achieved in this subtask is a method for closed-loop order reduction of parallel models with application to parallel working boilers. This result is described in [HPL5] and it is being prepared for publication. HPL used about 8MM on this subtask. An extension is being prepared in the joint KTH/HPL collaboration[KTH9]. KTH has also contributed with a new method for subspace identification of cascade systems [KTH6].

Second subtask, T3.1.2, addresses input signal design for identification. The optimal experiment design is a non-convex, and hence non-tractable problem. HPL proposed a novel method which is sub-optimal, but simple and tractable method and which results in designed input that can improve the overall model quality, while minimizing abruptions to identified system. This result is described in internal report [HPL4] and now it is in the patenting process. According to the plan, 5MM were spent at HPL on this task.

KTH has also made significant contributions to optimal input signal design. A very general applications oriented experiment design methodology has been developed. This has been published in [KTH1] and was presented in a Plenary Address at the European Control Conference 2009, Budapest, Hungary [KTH3] and in a Plenary Address at the Benelux meeting 2010 [KTH4]. This framework has been adapted to MPC oriented experiment design, details are provided in [KTH5, KTH8]. A key problem in all optimal experiment design procedures is that the solution depends on the unknown system parameters to be identified. An adaptive method to cope with this is presented in [KTH2] for ARX systems. The KTH lab has also developed an input design procedure for Multi-Input Multi-Output linear time-invariant systems based on a simplified model accuracy measure valid for highly complex (many estimated parameters) systems [KTH7]. The invited session “Optimal Experiment Design” is being submitted to the IFAC World Congress 2011. A further contribution has been input design for cascade systems, see Section 2.10.

The third subtask, T3.1.3, regards subspace ID for Large systems. HPL developed algorithms able to incorporate basic types of prior information (gains, time constants, ... to subspace identification methods. The results were published in [HPL1]. Also scalability aspects have been considered. Incorporating prior knowledge improves the posedness of the ID problem, which may be poor in cases of low input excitation. This is often the case of large-scale interconnected systems. In an additional development, a modification of the subspace ID for large-scale systems was proposed which uses better internal data representation and dramatically reduces memory requirements. Hence, the modified algorithm improves scalability of subspace ID methods. Another approach for grey-box identification was being developed in parallel. This approach is based on numerical optimization of mixed prediction and simulation error based criterion. The results were published in [HPL3] and [HPL6]. About 8MM were used on this task by HPL.

Subtask T3.1.4, regards failure detection in large-scale systems. 1MM was spent by HPL on this task. The results in this subtask are minor in correspondence with significantly limited time for this subtask.

WIDE Contributions related to D3.1

Honeywell, Prague Laboratory

Accepted Journal Papers

[HPL1] P. Trnka and V. Havlena. Subspace-like identification incorporating prior information. *Automatica*, 45(4):1086–1091, 2009.

Accepted Conference Papers

[HPL2] P. Trnka and V. Havlena. Overlapping models merging for large-scale model management. In *IEEE Conference on Systems and Control (IEEE MSC)*. IEEE, 2010.

[HPL3] J. Řehoř and V. Havlena. Grey-box model identification - control relevant approach. In *IFAC Workshop on Adaptation and Learning in Control and Signal Processing (IFAC ALCOSP)*. IEEE, 2010.

Technical Reports

[HPL4] P. Trnka and D. Pachner. Optimal input design - lqid. Technical report, Honeywell Prague Laboratory (HPL), Prague, 2009.

[HPL5] P. Trnka. Embedded parallel models order reduction. Technical report, Honeywell Prague Laboratory (HPL), Prague, 2010.

[HPL6] J. Řehoř. MACE Grey box modeling based id tool. Technical report, Honeywell Prague Laboratory (HPL), Prague, 2009.

KTH Automatic Control Laboratory

Accepted Journal Papers

[KTH1] H. Hjalmarsson. System identification of complex and structured systems. *European Journal of Control*, 15(4):275–310, 2009.

[KTH2] L. Gerencsér, H. Hjalmarsson, and J. Mårtensson. Identification of ARX systems with non-stationary inputs - asymptotic analysis with application to adaptive input design. *Automatica*, 45(3):623–633, March 2009.

Accepted Conference Papers

[KTH3] H. Hjalmarsson. System identification of complex and structured systems. In *European Control Conference*, pages 3424–3452, Budapest, Hugary, 2009. Plenary address.

[KTH4] H. Hjalmarsson. System identification of complex and structured systems. Parts I and II. In *Proceedings of the 29th Benelux meeting on Systems and Control 2010*, Plenary address. Kapellerput Heeze, The Netherlands, April 2010.

[KTH5] B. Wahlberg, H Hjalmarsson, and M. J. E. Annergren. On optimal input design in system identification for control. In *Proceedings 49th IEEE Conference on Decision and Control*, Atlanta, GA, USA, 2010.

[KTH6] P. Hägg, B. Wahlberg, and H. Sandberg. On subspace identification of cascade structured systems. In *Proceedings of the 49th IEEE Conference on Decision and Control*, Atlanta, GA, USA, 2010. To appear.

[KTH7] C. R. Rojas, H. Hjalmarsson, and R. Hildebrand. MIMO experiment design based on asymptotic model order theory. In *Proceedings IEEE Conference on Decision and Control*, Shanghai, China, 2009.

Technical Reports

[KTH8] C. Larsson an C.R. Rojas and H. Hjalmarsson. MPC oriented experiment design. 2010. Draft manuscript.

[KTH9] C. Sturk, P. Trnka, H. Sandberg, V. Havlena, and J. Řehoř. Closed-loop model reduction of parallel models. 2010. Draft. To be submitted to *IFAC World Congress 2011*.

2 Results Details

2.1 Unified model representation

The selection of Large Scale (LS) unified model representation is important step in WIDE project. The representation has to be simple for model management (applying updates to models and changes to model structure), model manipulations (order reductions, models merging) and efficient to support following model based design (distributed Kalman filtering, distributed model predictive control).

It is natural to represent LS system as a set of interconnected submodels. We chose to represent it by separating representation of submodels and representation of interconnection between submodels and external inputs and outputs (Figure 1). The subsystems are represented as a state space model *M* with block diagonal structure

$$M(s)=\left[\begin{array}{c|c} A_M & B_M \\ \hline C_M & D_M \end{array}\right], \quad \begin{array}{ll} A_M=\operatorname{diag}\{A_1,\ldots,A_n\}, & C_M=\operatorname{diag}\{C_1,\ldots,C_n\}, \\ B_M=\operatorname{diag}\{B_1,\ldots,B_n\}, & D_M=\operatorname{diag}\{D_1,\ldots,D_n\}. \end{array}$$

The submodels has stacked outputs denoted as *y* and stacked inputs denoted as *u*. The external inputs of LS model are denoted as *w* and external output as *z*. The interactions between submodels and between submodels and external inputs and outputs is described by static interconnection matrix L

$$\begin{pmatrix} z \\ u \end{pmatrix}=L\begin{pmatrix} w \\ y \end{pmatrix}, \qquad \begin{pmatrix} z \\ u \end{pmatrix}=\begin{pmatrix} L_{zw} & L_{zy} \\ L_{uw} & L_{uy} \end{pmatrix}\begin{pmatrix} w \\ y \end{pmatrix}.$$

The state space model of the whole LS model is

$$M_{full}(s)=\left[\begin{array}{c|c} A_M+B_M H L_{uy} C_M & B_M H L_{uw} \\ \hline L_{zy} G C_M & L_{zw}+L_{zy} D_M L_{uw} \end{array}\right], \quad H=\left(I-L_{uy}D_M\right)^{-1}, \quad G=\left(I-D_M L_{uy}\right)^{-1}$$

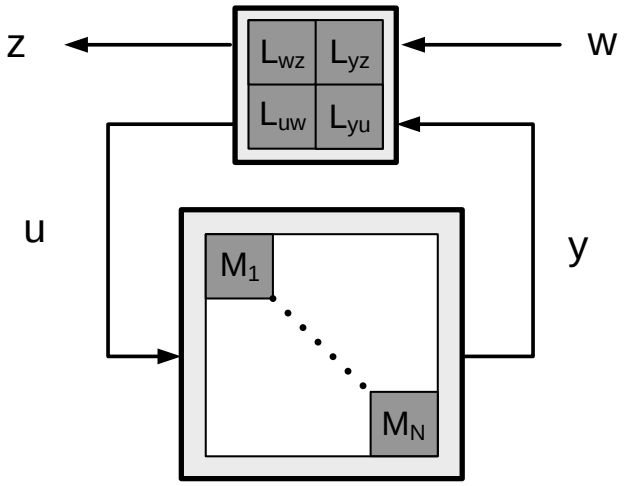

Figure 1 Internal Model Representation (w are external inputs and z are external outputs)

2.2 Models Merging

Large-scale system can be described by **mutually overlapping models**. Combining these models into global model needs solution to a problem, how to combine information from multiple models describing the same system.

Our solution assumes ARX or FIR models with normally distributed parameters and possibly different structural parameterization. It is obvious that direct merging of two ARX models in parameters is not possible as models can have different structure (different degrees of nominator / denominator and input delay). Merging in "parameters domain" has to be replaced by merging in time or frequency domain.

The merging in frequency domain is quite straightforward with apparent physical interpretation. However, the resulting uncertainty in frequency domain cannot be easily transformed back to uncertainty in ARX model parameters. On the other side, merging in time domain does not have this drawback. The merged model parameters are again described by mean value and covariance matrix.

Merging in time domain can be based on description of ARX model by **equivalent data**, which is input/output data set resulting to the same estimate of model parameters mean value and covariance.

Assume model parameters described by Normal distribution $\theta \sim N(\hat{\theta}, s^2 P)$, where $\hat{\theta}$ is mean value, *P* is normalized covariance and s^2 is normalization constant (residual variance). Finding equivalent data means to find regressor *Z* and RHS vector *b* such that

$$Z\hat{\theta} = b, \quad Z^T Z = P^{-1},$$

where *Z* and *b* have correct Hankel structure induced by ARX model.

Having equivalent data for each model makes merging simple as equivalent data can be reordered into regressor and RHS vector of any structure. Reordering equivalent data of all merged models into same structure of target model allows to stack the regressors and RHS vectors and compute final model parameters by weighted least squares (Figure 2).

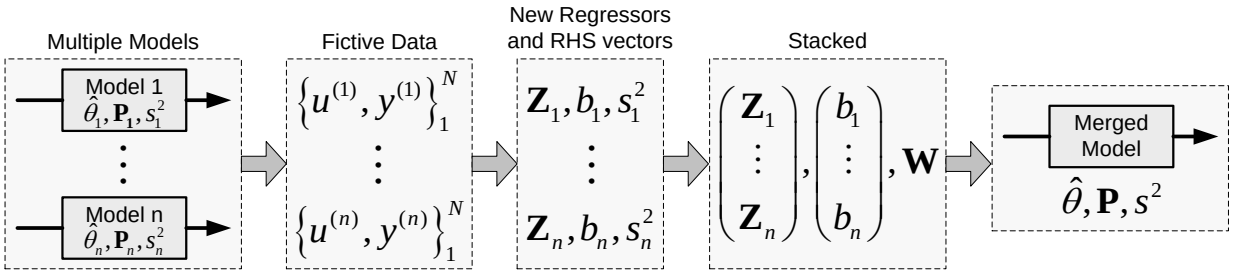

Figure 2 Models merging by equivalent data - algorithm block scheme.

The following example shows merging of three models of the same system, where the models were obtained from the experimental data with inputs on the different part of frequency spectra. The individual models are identified by PEM with ARX structure and data are generated by fourth order ARX system

$$\frac{B(s)}{A(s)} = \frac{\omega_1^2 \omega_2^2}{(s^2 + 2\omega_1\xi_1 s + \omega_1^2)(s^2 + 2\omega_2\xi_2 s + \omega_2^2)},$$

with $\omega_1 = 2,\ \omega_2 = 5,\ \xi_1 = 0.3,\ \xi_2 = 0.1$ discretized with $T_s = 0.2\,\mathrm{s}$. The frequency spectrum of experimental inputs for individual models is in Figure 3. The experimental data were obtained with signal to noise ratio of 30 dB. The length of identification data is 300 and the length of equivalent data (Figure 4) was selected as 50.

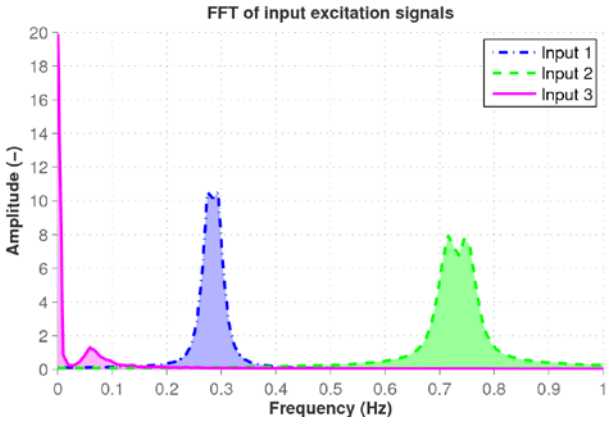

Figure 3 Frequency spectrum of inputs used to get identification data.

The properties of each model are summarized in the following table:

	Order	**Inputs Excitation**
Model 1	**2**	Around 1st resonance frequency
Model 2	**3**	Around 2nd resonance frequency
Model 3	**1**	Low frequencies

The mean values and variances of frequency characteristics of individual models and merged model are in Figure 5. It can be seen that merged model obtained by equivalent data takes the best information from individual models (the parts of frequency spectra with low variance) and combines it together into model which is close to original system (black dashed line).

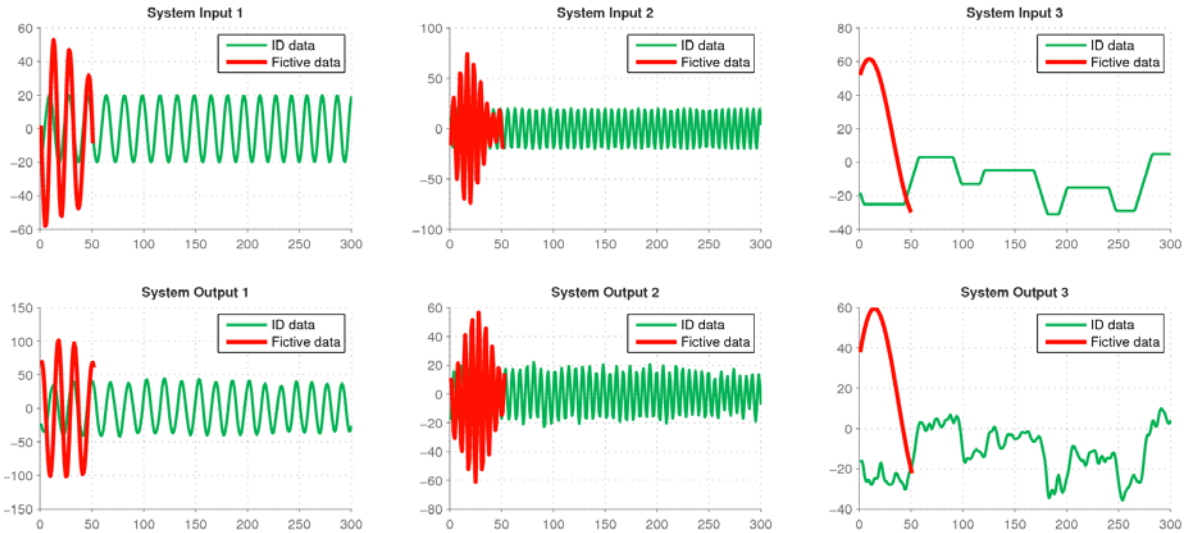

Figure 4 Data used for identification vs. equivalent (ficitive) data.

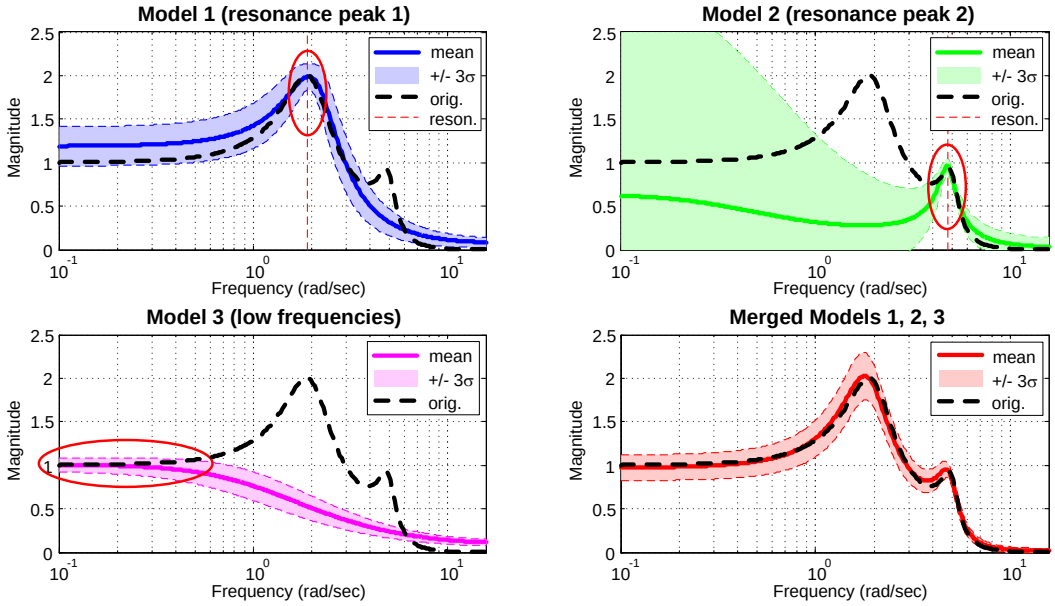

Figure 5 Merging of three models of 4th order system with two significant resonance frequencies. Each model is identified from data obtained on the different part of frequency spectra (highlighted by ellipse). The first 2nd order model is obtained from data around 1st resonance frequency, the second 3rd order model is obtained from data around 2nd resonance frequency and the third 1st order model is obtained from low frequency data.

More details, mathematical formulations and algorithm description can be found in attached publication [HPL2].

2.3 Consistent combination of interconnected models with uncertainty

Global model of large-scale system can be obtained by separated identification of individual subsystems followed by their combination into global model. The process of models combination must take into account not only the structure of models interconnection, but also the quality of individual models (variance of estimated model parameters) to guarantee the resulting model consistency.

Assume a set of single input and single output ARX or FIR models with normally distributed parameters connected in an arbitrary structure. The model of interconnected systems is a rational function, where coefficients of numerator and denumerator polynomials are given as sum of **convolutions** of vectors given by submodels numerators and denumerators.

Statistically correct mean value and variance of interconnected models needs an ability to compute **mean value and variance of multiple normal vectors convolution**. The exact result can be derived for two random vectors convolution by using relations for expectations of quadratic and quartic forms. Convolution of multiple vectors is obtained by sequential use of the result for two vectors.

The mean values of resulting model parameters can be also obtained by using only mean values of sub-models parameters and ignoring their covariance. However, this can be shown to give biased results, which would bring inconsistency into large-scale model management platform. Moreover, this bias would be more significant in case of mutually correlated parameters of submodels, which can arise from decomposition of multiple inputs / multiple outputs model into a set of single input / single output models.

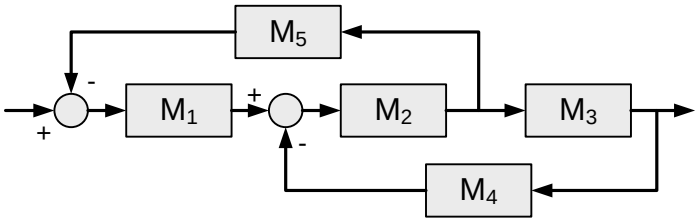

Figure 6 Models interconnection structure of example

Low complexity example with connection of five uncertain models is in Figure 6. Models M1, M4, M5 are of the 2nd order and models M2, M3 are of the 1st order with mutually correlated normal coefficients. The level of uncertainty is exaggerated to demonstrate the difference between statistically correct computations (denoted as "Proper Connection") and computations with mean values only (denoted as "Simple Connection"). Comparison of the result obtained by ignoring models uncertainty and by proper models connection is in Figure 7 and Figure 8.

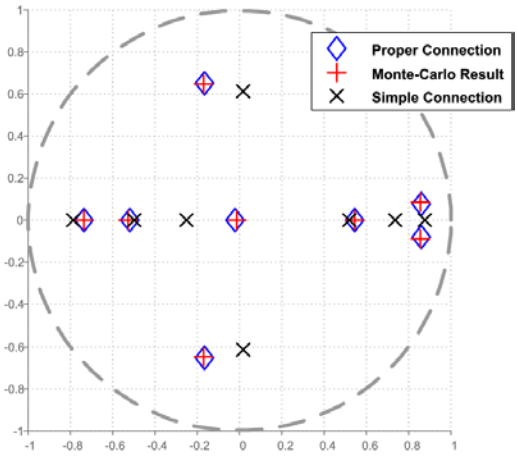

Figure 7 Global model poles position – comparison of results obtained by Monte Carlo simulations, statistically consistent combination and combination using only submodel mean values

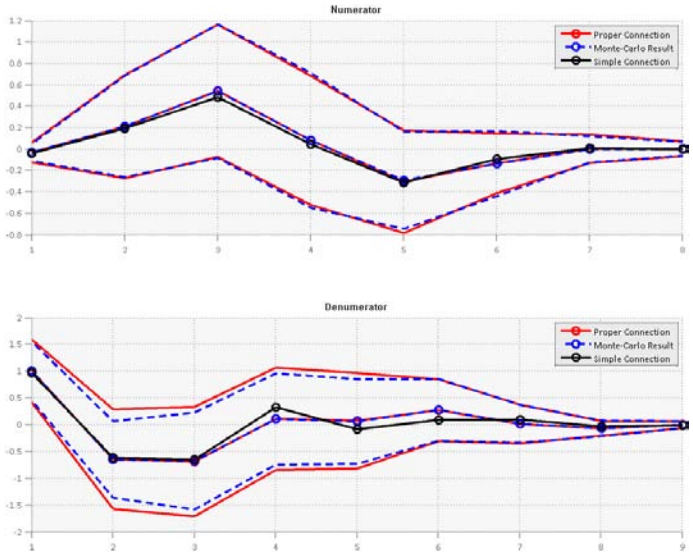

Figure 8 Mean values and standard deviation of numerator and denumerator vector of coefficient. Comparison of reuslt obtained by Monte-Carlo simulation (blue), proper connection based on random vectors convolution (red) and mean value obtained by ignoring submodel parameters covariances (black).

More details, mathematical formulations and algorithm description can be found in attached publication [HPL2].

2.4 Subspace Identification with Prior Information

The Subspace State Space System IDentification (4SID) has shown its suitability for industrial applications (Favoreel, De Moor, & Van Overschee, 2000), mainly due to its numerical robustness and the ability to identify MIMO (Multiple Inputs Multiple Outputs) systems with the same complexity as that for SISO (Single Input Single Output) systems without a need for extensive structural parameterization. However, it is quite usual that input/output data obtained from identification experiments in the industrial environment do not always have sufficient quality to give a good model by themselves. This may be caused by the fact that process excitation during identification experiments is limited by economical and safety reasons, which often results in data without proper excitation and with strong noise contamination. The black-box approach as in 4SID, relying only on experimental data, may provide biased models in such cases. In practical applications there is often strong prior information (PI) about the system, which can be exploited by the identification algorithm to improve the quality of the identified model. Such information can be approximate knowledge of time constants, known static gains, an input/output stability, step response smoothness, etc. It can be obtained from process operator experience, first principles model, by the analysis of process history data, etc.

The proposed algorithm uses the interpretation of subspace identification as an optimization problem of finding a model as an optimal multi-step predictor (Van Overschee & De Moor, 1996) for the experimental data. Further, the problem is reformulated in the Bayesian framework allowing a combination of available PI with information from the experimental data.

Algorithm Outline

This section shows an overview of the algorithm. The algorithm is based on a class of subspace identification methods. However, these methods use algebraic oblique/orthogonal projections, QR/SVD factorization and thus incorporation of additional knowledge is not straightforward. We are using similarity of SIM with optimization of multi-step predictor on experimental data. There are four main steps:

1) **Construction of multi-step predictor data matrices**. The assumed model is a bank of conjugated linear time invariant predictors with certain special structure ensuring causality and avoiding parameter redundancy. The model is parameterized by Kalman filter parameters and impulse response elements and uses two windows of past and future data of certain lengths.
2) Real-world prior information is transformed to **prior estimate of multi-step predictor impulse response in the form of mean value and covariance matrix**.
3) The posterior mean value and covariance matrix of impulse response is estimated using **Bayesian inference**, i.e. combining information from experimental data with prior information.
4) The state space model is realized from the mean value and covariance matrix of impulse response by **structure weighted low rank approximation** (SWLRA).

The block scheme of the algorithm is in **Figure 9**.

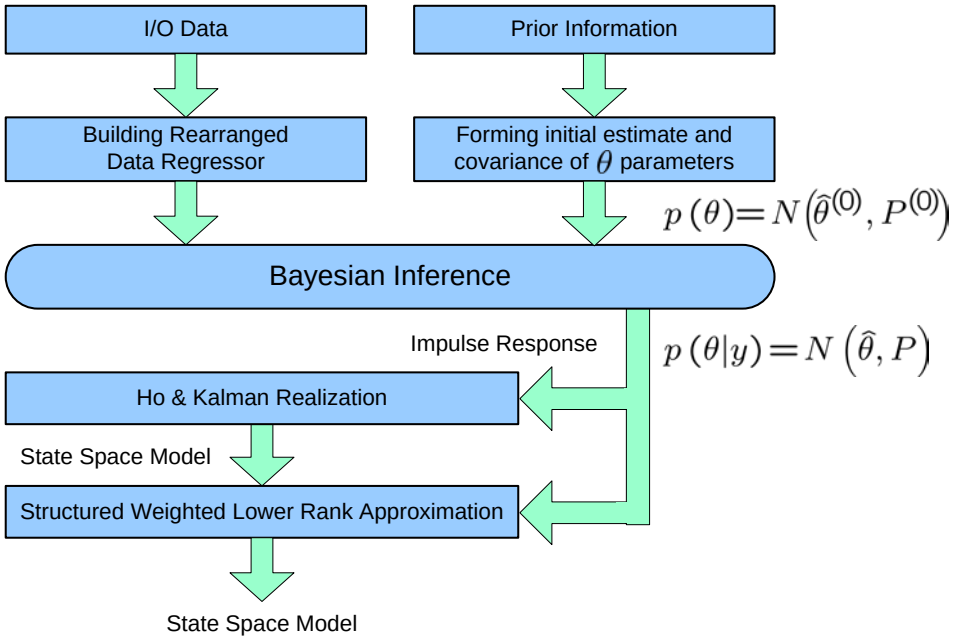

Figure 9: Algorithm block diagram.

Example – Oil-fired Steam Boiler

Description: Experimental data were collected from oil-fired steam boiler (Figure 7) on the set point of 95% boiler rated power. The goal is to identify model relating fuel and steam demand to boiler steam pressure. This system is simple; however, it is well known identification problem [7], where fuel and steam demand inputs are typically strongly collinear, because technological limitations do not allow independent excitation of each input.

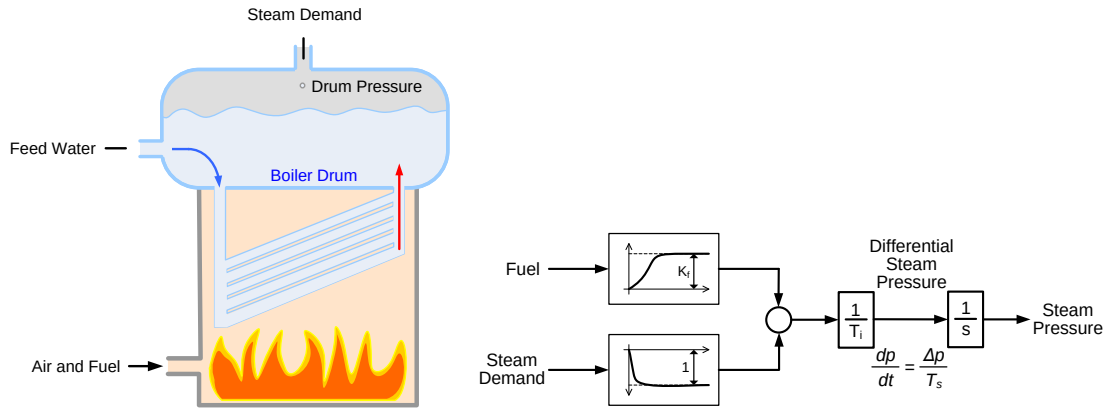

Figure 10: Oil-fired boiler scheme and model scheme.

The I/O data are on the following figure.

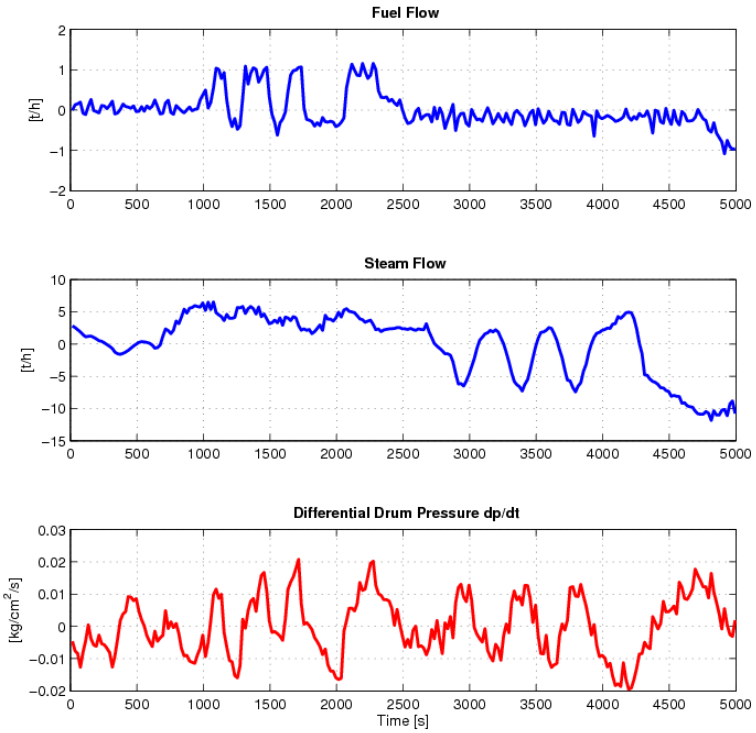

Figure 11: Experimental I/O data for identification.

Identification: The system was identified by our algorithm and compared to models from N4SID and PEM with ARX and ARMAX model structure. The prior information used for identification was:

- known relative gain between (fuel flow -> drum pressure) and (steam demand -> drum pressure) – amount of steam units generated from one unit of fuel Fuel2Steam=12.08
- fast response from steam demand to steam pressure
- enforced smoothness
- no direct feed through (h(0)=0)

Results: Even though the model identified by P4SID is more restricted due to constraints imposed by prior information it gives best fit factor and obviously complies with prior information.

The fit factors for identified models compared to the output of deterministic subsystem are following

Method	**Model Order**	**Fit Factor**	**Relative Gain (correct value 12.08)**
P4SID	2	32 %	12.04
N4SID	2	20 %	7.85
ARX	$(2 \quad 2)$	24 %	9.93
N4SID	$(2 \quad 2)$	19 %	14.52

The model step responses are in **Figure 12**.

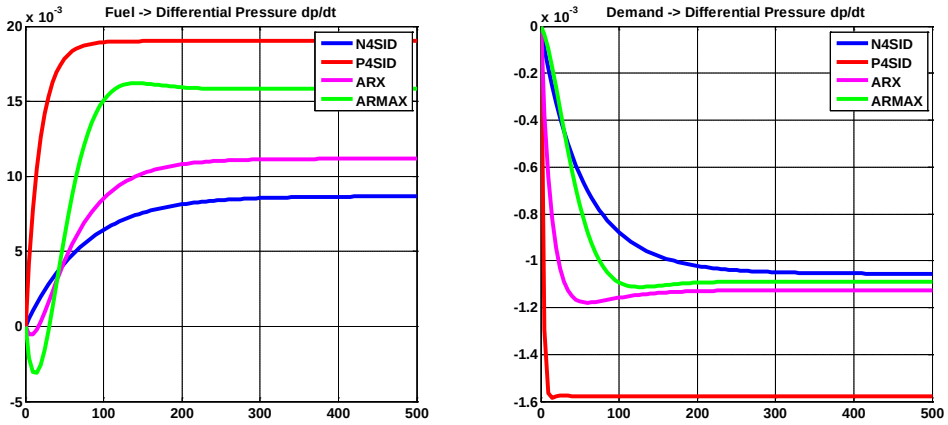

Figure 12: Step responses of models obtained by different algorithms.

More details, mathematical formulations and algorithm description can be found in attached publication [HPL1].

2.5 Large-scale Subspace Identification

Algorithms of Subspace Identification Methods (SIM) compute with **highly redundant matrices** (mainly Hankel matrices constructed from input / output data). Size and computational needs of these redundant matrices **limit the usability of SIM** on long data sets or a data sets from large-scale multiple inputs / multiple outputs systems.

Standard SIM algorithm can be modified to parsimonious versions, which work only with vectors of stacked input / output data and do not create Hankel or other redundant matrices.

The following table shows standard MOESP algorithm (left column) and our parsimonious modification (right column).

MOESP	Parsimonious MOESP
Hankel matrices (i rows) $u \to U,\ y \to Y$	Covariance matrices (without forming U,Y) $P_{uu} = UU^T, P_{uy} = UY^T, P_{yy} = YY^T$
Orthogonal projection (LQ factorization) $\begin{pmatrix} U \\ Y \end{pmatrix} = \begin{pmatrix} L_{11} & 0 \\ L_{21} & L_{22} \end{pmatrix} \begin{pmatrix} Q_1 \\ Q_2 \end{pmatrix} \Rightarrow Y/U^{\perp} = L_{22}Q_2$	Cholesky factorization $\begin{pmatrix} U \\ Y \end{pmatrix} \begin{pmatrix} U \\ Y \end{pmatrix}^T = \begin{pmatrix} P_{uu} & P_{uy} \\ P_{uy}^T & P_{yy} \end{pmatrix} = \begin{pmatrix} L_{11} & 0 \\ L_{21} & L_{22} \end{pmatrix} \begin{pmatrix} L_{11}^T & L_{21}^T \\ 0 & L_{22}^T \end{pmatrix}$
Extended observability matrix $L_{22} \to (SVD) \to \Gamma_i$	—— || ——
Parameters A,C estimation $\underline{\Gamma_i} A = \overline{\Gamma_i}, \quad C = \Gamma_i(1:\ell,:)$	—— || ——
Parameters B,D estimation $\Gamma^{\perp} Y U^{+} \ \to$ set of equations linear in B,D	Parameters B,D estimation (proper excitation) $\Gamma^{\perp} Y U^{+} = \Gamma^{\perp} Y U^T (UU^T)^{-1} = \Gamma^{\perp} P_{uy}^T P_{uu}^{-1}$ $\Gamma^{\perp} P_{uy}^T P_{uu}^{-1} \to$ set of equations linear in B,D

The difference in memory consumption is significant as Cholesky factors of parsimonious MOESP (needed to get final results) can be computed without forming Hankel matrices *U* and *Y*.

2.5.1 Scalability of Large-scale Subspace Identification

The scalability of Parsimonious and Standard MOESP methods can be evaluated in the terms of computational complexity and memory demands. The practical implementation of both algorithms requires the following matrix algorithms (with different matrix sizes)

Standard MOESP:

Algorithm Step	Matrix Algorithm
1) Forming Hankel matrices from data	
2) Orthogonal Projection	Orthogonal triangularization
3) Extended Observability matrix extraction	Gram-Schmidt orthogonalization
4) Parameters A,C estimation	LS solution by QR factorization
5) Parameters B,D estimation	LS solution by QR factorization

Parsimonious MOESP:

Algorithm Step	Matrix Algorithm
1) Covariance matrices computation	
2) Covariance Cholesky factorization	Cholesky factorization
3) Extended Observability matrix extraction	Gram-Schmidt orthogonalization
4) Parameters A,C estimation	LS solution by QR factorization
5) Parameters B,D estimation	LS solution by QR factorization (reduced problem in comparison to standard MOESP)

The computational complexity of the required algorithms is following table (taken from G.W. Steward, Matrix Algorithms, 1998). The complexity is measured in FLAMs, which is the number of floating point additions and multiplications.

Matrix Algorithm	Computational Complexity (FLAM)
Orthogonal triangularization $\mathbf{A} \in \mathbf{R}^{n \times p}$, $\mathbf{QA} = \begin{pmatrix} \mathbf{R} \\ 0 \end{pmatrix}$	$np^2 - \frac{1}{3} p^3$
Cholesky factorization $\mathbf{A} \in \mathbf{R}^{n \times n}$	$n^3 / 6$
Gram-Schmidt orthogonalization $\mathbf{A} \in \mathbf{R}^{n \times p}$	$np^2 - \frac{1}{3} p^3$
LS solution by QR factorization $\mathbf{A} \in \mathbf{R}^{n \times p}$, $\mathbf{Ax} = \mathbf{b}$	$6np^2$ for $n >> p$

Assume system with m inputs, ℓ outputs and identification data set with N_S samples and subspace "horizon" length as j. The main difference between standard and parsimonious algorithm is in the orthogonal triangularization versus Cholesky factorization

Standard MOESP	***Parsimonious MOESP***
Orhogonal triangularization (step 2)	Cholesky factorization (step 2)
$NP^2 - \frac{1}{3} P^3$	$\frac{1}{6} P^3$
N … approximately the number of data samples, $N \doteq N_S$. P … number of Hankel data matrices rows, $P = (m + \ell)\, j$.	

Typically $N >> P$ and therefore $NP^2 - \frac{1}{3}P^3 >> \frac{1}{6}P^3$.

and significantly different sizes of matrices in the last LS problem

Standard MOESP	*Parsimonious MOESP*
LS solution by QR (step 5)	LS solution by QR (step 5)
$6NP_U^2$	$\sim 6P_U^3$
P … number of input Hankel data matrices rows, $P_U = mj$.	
Typically $N >> P$ and therefore $6NP_U^2 >> 6P_U^3$.	

The main difference in memory demands is the need of standard MOESP to form Hankel data matrices, where the number of matrix elements is approximately $(m+\ell)jN$.

The comparison of both algorithms scalability as a function of system size (number of inputs and outputs) is in Figure 13. Left figure shows computational complexity and right figure shows memory demands for 10th order system. A similar comparison of both algorithms scalability as a function of number of data samples is in Figure 14.

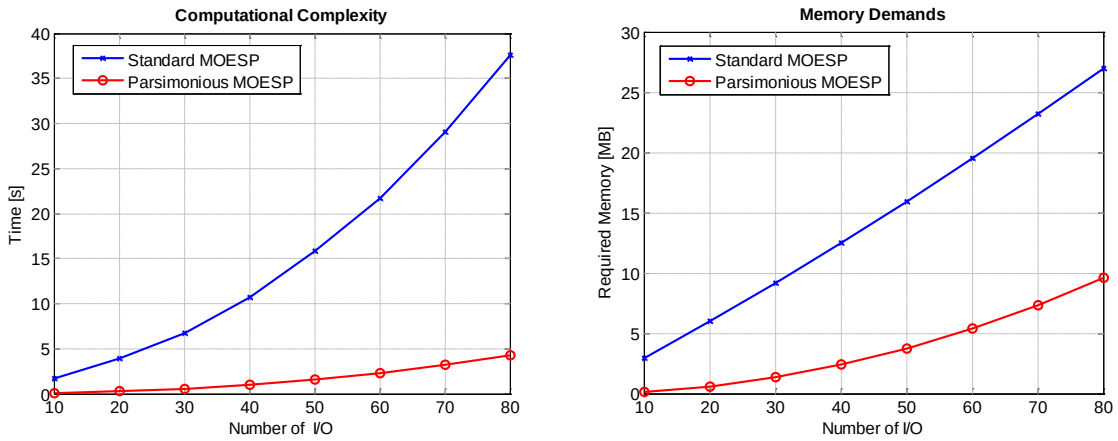

Figure 13 Computational complexity and memory demands as a function of a number of inputs and outputs (10th order system, 10^4 number of samples).

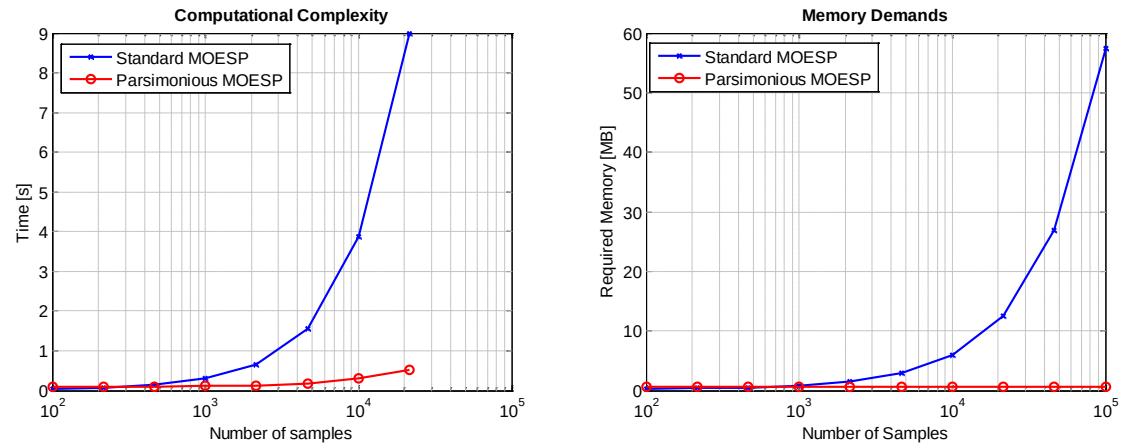

Figure 14 Computational complexity and memory demands as a function of number of samples (10th order system with 10 inputs and 10 outputs).

2.6 Grey-box identification

Grey-box modeling is an advantageous tool for system identification where available input/output experimental data are insufficiently excited. The lack of information in the data can be often improved with additional knowledge about the modeled system, which constricts the class of models under consideration. The real system is usually more complex and do not fit the model class, thus a bias error occurs. The main goal of our effort was to find an effective way to identify grey-box models, which would be relevant in commissioning predictive control.

In our approach, we use a combination of two models, Output Error and ARMAX. Both models have the same deterministic part (conveniently parameterized space model), which is described trough the grey-box modeling, but noise filters are different. Using prediction error identification (PEM) approach, the Output Error model optimizes parameters with respect to the open-loop predictions, whereas the ARMAX model is focused on one-step predictions. Both, open-loop output predictions and one-step output predictions are effectively mixed in non-linear least square optimization criterion to find a model with improved deterministic part.

More details, mathematical formulations and algorithm description can be found in attached publication [HPL3] and [HPL6].

2.7 Parallel models closed-loop order reduction

Most large-scale industrial processes can be viewed as an interconnection of MIMO subsystems. It is quite frequent that a subset of these subsystems is working in parallel (Figure 13) – for example a set of boilers feeding a single header, a set of pumps, turbines, chemical reactors, etc. These parallel sub-systems can be operated in a multiple on/off configurations according to demands and allocation optimization. Design of Advanced Process Control (APC) has to consider this multiplicity and requires global model for every possible configuration. For example, MPC with model switching requires models, which are usually obtained by individual step testing.

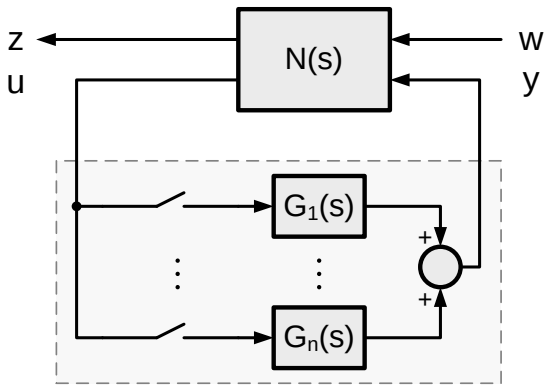

Figure 15 Parallel working subsystems as a part of large-scale system.

Assume that the models of all subsystems are identified – state space models with a set of parameters (with physical interpretation) adjusted from experimental data. It is highly desirable to construct global models with reduced order. However, for a reasonable design of KF and MPC it is also important to preserve physical meaning to the most of model states and interconnection signals (KF and MPC tuning and constraints specification). These contradictory requirements can be fulfilled by reducing only the parallel models, as their functionality is similar. The advantage is that the controller can then be designed for each configuration such as if there is a single system with variable parameters instead of variable number of parallel systems.

Motivating industrial example is a set of boilers feeding a common header. Typically, fuel flow of all boilers is operated by a common signal. Each boiler (Figure 14) can be with significant simplification described by internal boiler volume and hydrodynamic pipe resistance between boiler and common header. There is also dynamics from fuel flow to generated steam, which is “normalized” by local combustion controller (to avoid oscillations / pushing among the parallel units).

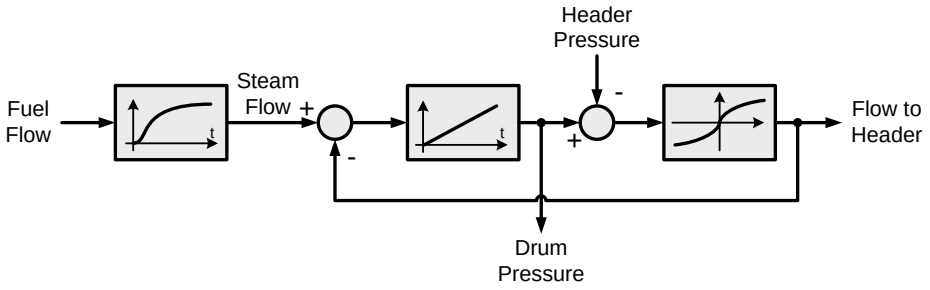

Figure 16 Boiler Block Scheme.

Low order models can be obtained by performing experiments for all possible on/off combinations and then fitting reduced order model or by using certain heuristics for parallel models reduction. Performing experiments for all combinations is not practical as the number of combinations can typically exceed tens / hundreds for larger solutions.

Model reduction is currently done by the following *heuristic* (based on the first principles). The parallel boilers are replaced by a single boiler with normalized fuel flow to steam flow dynamics, drum volume is computed as a sum of individual boiler drum volumes and pipe resistance is computed as parallel resistance of individual boiler pipe resistances.

Although described heuristic works quite well for boilers it would be preferable to replace it by a systematical approach such as balanced order reduction. Straightforward naive application of balanced reduction to parallel models and integration of reduced model to global model can give significantly biased and even unstable global model. The problem is that the “local” reduction of parallel models has to be done with respect to global model. This can be achieved by the algorithm of structured balanced reduction proposed in
Henrik Sandberg, Richard M. Murray: "Model reduction of interconnected linear systems". Optimal Control, Applications and Methods, Special Issue on Directions, Applications, and Methods in Robust Control, 30:3, pp. 225-245, May/June 2009,
where an optimal order reduction of parallel models is achieved with the lowest degradation of global model (the measure of degradation is models difference inf norm).

Problem summary:

- Large-scale system with sub-system of parallel working sub-systems
- Individual parallel subsystems can be switched on/off
- Global model for each potential on/off combination is needed with the following requirements:
    - order of parallel connected models is reduced (optimally from global model view)
    - physical interpretation of non reduced subsystems has to be preserved to allow convenient design of KF and MPC and for specification of constraints on internal states

Algorithm

The algorithm is simplified algorithm for structure preserving balanced order reduction. The simplification is that there is only a single system $G(s)$ for reduction (Figure 15b) compared to multiple systems $G_1(s),\ldots,G_q(s)$ considered in general structure preserving balanced order reduction algorithm (Figure 15a).

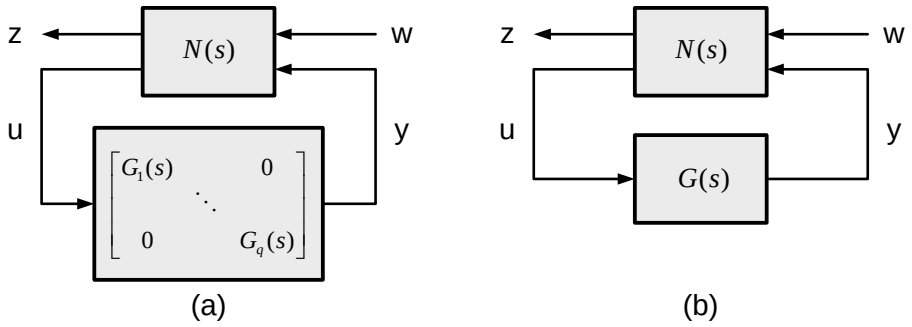

Figure 17 Structure preserving order reduction block scheme (a). Globally optimal local model reduction (b).

Parallel systems model ..... $G(s) = \left[\begin{array}{c|c} A_G & B_G \\ \hline C_G & D_G \end{array}\right]$

Remaining model ..... $N(s) = \left[\begin{array}{c|cc} A_N & B_{N,1} & B_{N,2} \\ \hline C_{N,1} & D_E & D_F \\ C_{N,2} & D_H & D_K \end{array}\right]$

External input ..... w
External output ..... z
Internal input ..... u
Internal output ..... y

Global state space model A, B, C, D with input w and output z can be computed as

$$\left[\begin{array}{c|c} A & B \\ \hline C & D \end{array}\right] = \left[\begin{array}{cc|c} A_N + B_{N,2}LD_GC_{N,2} & B_{N,2}LC_G & B_{N,1} + B_{N,2}LD_GD_H \\ B_GMC_{N,2} & A_G + B_GMD_KC_G & B_GMD_H \\ \hline C_{N,1} + D_FD_GMC_{N,2} & D_FLC_G & D_E + D_FD_GMD_H \end{array}\right], \quad \text{where} \quad \begin{array}{l} L := \left(I - D_GD_K\right)^{-1}, \\ M := \left(I - D_KD_G\right)^{-1}. \end{array}$$

Controllability Gramian P and observability Gramian Q are computed for global model and separated as

$$P = \begin{pmatrix} P_N & P_{NG} \\ P_{NG}^T & P_G \end{pmatrix}, \quad Q = \begin{pmatrix} Q_N & Q_{NG} \\ Q_{NG}^T & Q_G \end{pmatrix}.$$

P_G and Q_G are used to compute globally optimal balancing transformation fro parallel models state vector $x_G = T\hat{x}_G$ (where $\hat{x}_G$ is reduced state vector for model $G(s)$) by standard balanced reduction algorithm:

1) computing Cholesky factor R of controlability Gramian $P_G = RR^T$
2) computing singular value decomposition $R^TQ_GR = U\Sigma^2U^T$
3) transformation T is computed as $T = RU\Sigma^{-1/2}$

Balancing subsystem $G(s)$

$$\hat{A}_G = T^{-1}A_GT = \begin{pmatrix} \hat{A}_{11} & \hat{A}_{12} \\ \hat{A}_{21} & \hat{A}_{22} \end{pmatrix}, \quad \hat{B}_G = T^{-1}A_GT = \begin{pmatrix} \hat{B}_1 \\ \hat{B}_2 \end{pmatrix},$$
$$\hat{C}_G = CT = \begin{pmatrix} \hat{C}_1 & \hat{C}_2 \end{pmatrix}, \qquad \hat{D} = D.$$

Obtaining reduced subsystem $\overline{A}_G, \overline{B}_G, \overline{C}_G, \overline{D}_G$ either by truncation

$$\bar{A}_G = \hat{A}_{11}, \quad \bar{B}_G = \hat{B}_1,$$
$$\bar{C}_G = \hat{C}_1, \quad \bar{D}_G = \hat{D}.$$

or by singular perturbation

$$\bar{A}_G = \hat{A}_{11} - \hat{A}_{12}\hat{A}_{22}^{-1}\hat{A}_{21}, \quad \bar{B}_G = \hat{B}_1 - \hat{A}_{12}\hat{A}_{22}^{-1}\hat{B}_2,$$
$$\bar{C}_G = \hat{C}_1 - \hat{C}_2\hat{A}_{22}^{-1}\hat{A}_{21}, \quad \bar{D}_G = \hat{D} - \hat{C}_2\hat{A}_{22}^{-1}\hat{B}_2.$$

Reduced order global model model is then

$$\left[\begin{array}{c|c} \hat{A} & \hat{B} \\ \hline \hat{C} & \hat{D} \end{array}\right] = \left[\begin{array}{cc|c} A_N + B_{N,2}L\bar{D}_G C_{N,2} & B_{N,2}L\bar{C}_G & B_{N,1} + B_{N,2}L\bar{D}_G D_H \\ \bar{B}_G M C_{N,2} & \bar{A}_G + \bar{B}_G M D_K \bar{C}_G & \bar{B}_G M D_H \\ \hline C_{N,1} + D_F\bar{D}_G M C_{N,2} & D_F L\bar{C}_G & D_E + D_F\bar{D}_G M D_H \end{array}\right], \quad \text{where} \quad \begin{array}{l} L := \left(I - \bar{D}_G D_K\right)^{-1}, \\ M := \left(I - D_K \bar{D}_G\right)^{-1}. \end{array}$$

Note:
Balanced reduction can be used only for strictly stable systems. This is usually circumvented by separating the system into strictly stable and the remaining part (for example by transformation to Jordan canonical form). However, this transformation / separation would inevitably destroy physical meaning of states, as it has to be applied to global model (even to parts we do not need to reduce).

Example – Parallel Boilers
Following simulations assumes 3 boilers feeding steam to a single header (Figure 6).

Linearized Boiler Model

$$A_i = \begin{pmatrix} -1/T_i & 0 \\ 1/V_i & -K_i/V_i \end{pmatrix}, \quad B_i = \begin{pmatrix} K_s & 0 \\ 0 & K_i/V_i \end{pmatrix}, \qquad u = \begin{pmatrix} p \\ FF \end{pmatrix} \quad \begin{array}{l} \ldots \text{header pressure} \\ \ldots \text{fuel flow} \end{array}$$
$$C_i = \begin{pmatrix} 0 & K_i \end{pmatrix}, \qquad D_i = \begin{pmatrix} 0 & -K_i \end{pmatrix}, \qquad y = SF \quad \ldots \text{steam flow to header}$$

where
V_i ..... i-th boiler volume
K_i ..... i-th boiler pipe to header conductivity
K_S ..... units of stem from unit fuel
T_i ..... i-th boiler 1st order time constant for fuel flow -> steam flow

Linearized header model

$$A_h = \begin{pmatrix} 0 \end{pmatrix}, \quad B_h = \begin{pmatrix} 1/V_H & -1/V_H \end{pmatrix},$$
$$C_h = \begin{pmatrix} 1 \end{pmatrix}, \quad D_h = \begin{pmatrix} 0 & 0 \end{pmatrix},$$

$$u = \begin{pmatrix} SF \\ SD \end{pmatrix} \quad \begin{array}{l} \ldots \text{steam flow to header} \\ \ldots \text{steam demand} \end{array}$$
$$y = p \quad \ldots \text{header pressure}$$

where
V_H ..... header volume
The parameters were chosen as

$$K_s = 10, \quad V = \begin{pmatrix} 300 & 500 & 700 \end{pmatrix}, \quad K = \begin{pmatrix} 100 & 130 & 150 \end{pmatrix}, \quad V_H = 100.$$

The global model has inputs Fuel Flow (FF) and Steam Demand (SD) and outputs Drum pressure (p) and overall Stem Flow to header (SF).

Simulations compare global model step responses for models obtained by:

- Naive (local) order reduction inserted into global model (green color)

- Structured reduction (red color)
- Global balanced reduction ignoring / damaging structure (blue color)

The results for truncation are in Figure 17. It can be seen that naive balanced reduction has large bias and tends to be unstable. The structure-preserving algorithm gives consistent results with minimized degradation to full order model.

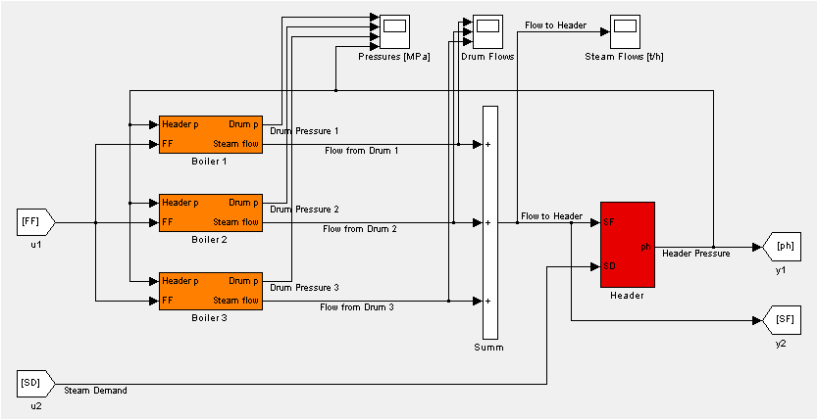

Figure 18 Parallel boilers feeding a single header

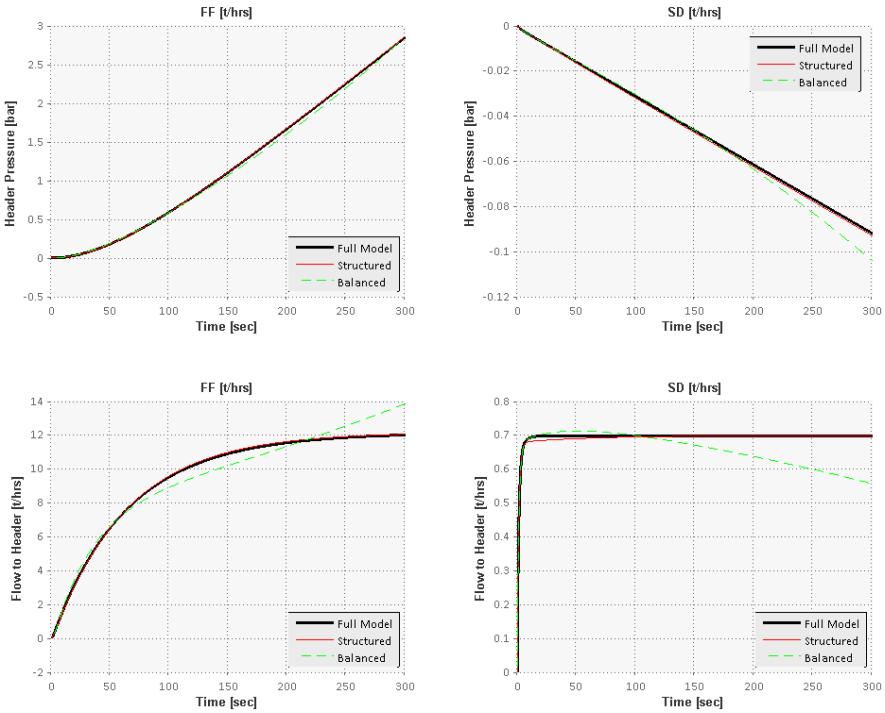

Figure 19 Reduced Models Step Responses

More details, mathematical formulations and algorithm description can be found in attached publication [HPL5].

2.8 Optimal Experiment Design

Optimal input design for identification is a difficult non-convex problem, which needs to be simplified in order to become tractable. The simplification used in our approach is that in each sampling period two models are selected from parameters uncertainty p.d.f., such that discriminating between these two models would bring the largest improvement in the model quality (improvement in parameters variance or control oriented model quality criterion). The input trajectory is then designed to cause the largest difference on the outputs of selected models, which would allow to efficiently distinguish between them.

The input design is based on a **relaxed LQ controller** (further denoted as LQID), which allows limited deviation from LQ optimal input trajectory. This degree of freedom is used for perturbation causing the largest output difference between two models selected from the uncertainty. Besides, of standard LQ weight parameters there is a single additional parameter *k* for continuous adjustment of the amount of additional energy used for the identification - setting this parameter to zero forces LQID to behave like LQ controller. LQID starts with preliminary model p.d.f., which is updated with each new I/O data pair and used for input design.

Relaxed LQ controller is based on standard LQ control criterion

$$J(u) = \sum_{\tau=t}^{\infty} x_\tau^T Q x_\tau + x_\tau^T S u_\tau + u_\tau^T R u_\tau,$$

with parameters *Q,S,R*. Price for the optimal control from state x_t is given by Bellman function

$$V_t = x_t^T P x_{t,}$$

where *P* is the solution of algebraic Riccati equation. According to the optimality principle the LQ optimal input trajectory $\overline{u}$ satisfies

$$J(\overline{u}_t^{t+h-1}) + V_{t+h} \le V_t$$

where *h* is the length of horizon. This equivalence constraint can be relaxed to allow certain degree of freedom for identification optimal perturbation

$$J(u_t^{t+h-1}) + V_{t+h} \le V_t + k, \qquad k \in \langle 0, \infty)$$

where *k* is the parameter for continuous adjustment of the amount of additional energy used for the identification. The Lyapunov stability of relaxed LQ controller can be easily proved.

Relaxed LQ controller can be realized as **quadratic optimization constraint**. Denoting

$$\mathbf{U} = \begin{pmatrix} u_t \\ \vdots \\ u_{t+h-1} \end{pmatrix}, \mathbf{X} = \begin{pmatrix} x_t \\ \vdots \\ x_{t+h-1} \\ x_{t+h} \end{pmatrix},$$

$$\bar{\mathbf{Q}} = \begin{pmatrix} \mathbf{Q} & & & \\ & \ddots & & \\ & & \mathbf{Q} & \\ & & & \mathbf{P} \end{pmatrix}, \bar{\mathbf{R}} = \begin{pmatrix} \mathbf{R} & & \\ & \ddots & \\ & & \mathbf{R} \end{pmatrix}, \bar{\mathbf{S}} = \begin{pmatrix} \mathbf{S} & & \\ & \ddots & \\ & & \mathbf{S} \\ 0 & \dots & 0 \end{pmatrix},$$

The quadratic constraint can be written as

$$\mathbf{U}^T \mathbf{H}_2 \mathbf{U} + f_2^T \mathbf{U} + c_2 \le 0, \qquad \text{where} \quad \begin{aligned} \mathbf{H}_2 &= \mathbf{N}^T \bar{\mathbf{Q}} \mathbf{N} + \mathbf{N}^T \bar{\mathbf{S}} + \bar{\mathbf{R}}, \\ f_2^T &= 2 x_t^T \mathbf{M}^T \bar{\mathbf{Q}} \mathbf{N} + x_t^T \mathbf{M}^T \bar{\mathbf{S}}, \\ c_2 &= x_t^T \mathbf{M}^T \bar{\mathbf{Q}} \mathbf{M} x_t - x_t^T \mathbf{P} x_t - k. \end{aligned}$$

LQID experiment design

The degree of freedom obtained by relaxed LQ is used to inject signal, which is optimal for differentiation between two models, which are selected from parameters p.d.f. as two models with largest uncertainty and large probability. The resulting optimization problem is quadratic programming with minimization of negative definite quadratic function and quadratic constraints.

Example of optimal signal to distinguish two models

LQID is applied to system

$$G(s) = \frac{\omega^2}{s^2 + 2\omega\xi s + \omega^2}, \quad \omega = 0.2\pi, \quad \xi = 1.$$

Two models, which need to be distinguished, are fixed to the same model with parameters

$$\text{S1:} \qquad \omega = 0.2\pi, \quad \xi = 1,$$

$$\text{S2:} \qquad \omega = 0.2\pi, \quad \xi = 0.05.$$

The optimal input signal computed by relaxed LQ to distinguish between model is in Figure 18 compared to result of a plain LQ controller.

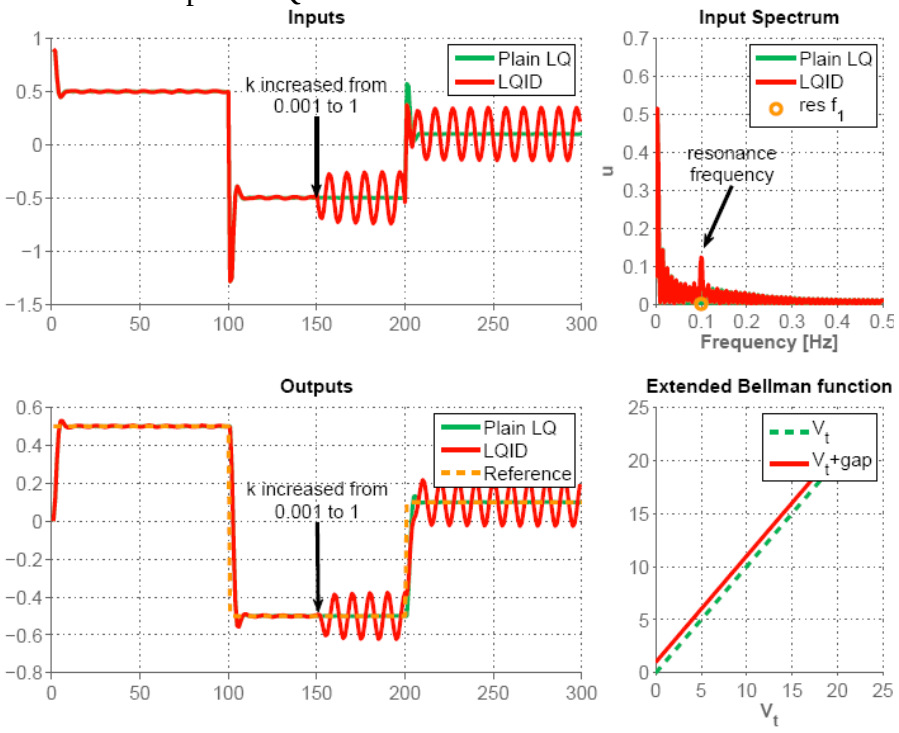

Figure 20 LQID with fixed selected model. The eneregy to additive identification signal is increased in t=150.

Identification with LQID

Two models are selected in each sampling period from the direction of the largest parameters variance (Figure 19). Energy limit for perturbation is reduced in t=160. Note the quality of step reference tracking in t=200. Can be used for closed loop identification, where model quality monitoring (predictions monitoring) initiates re-identification.

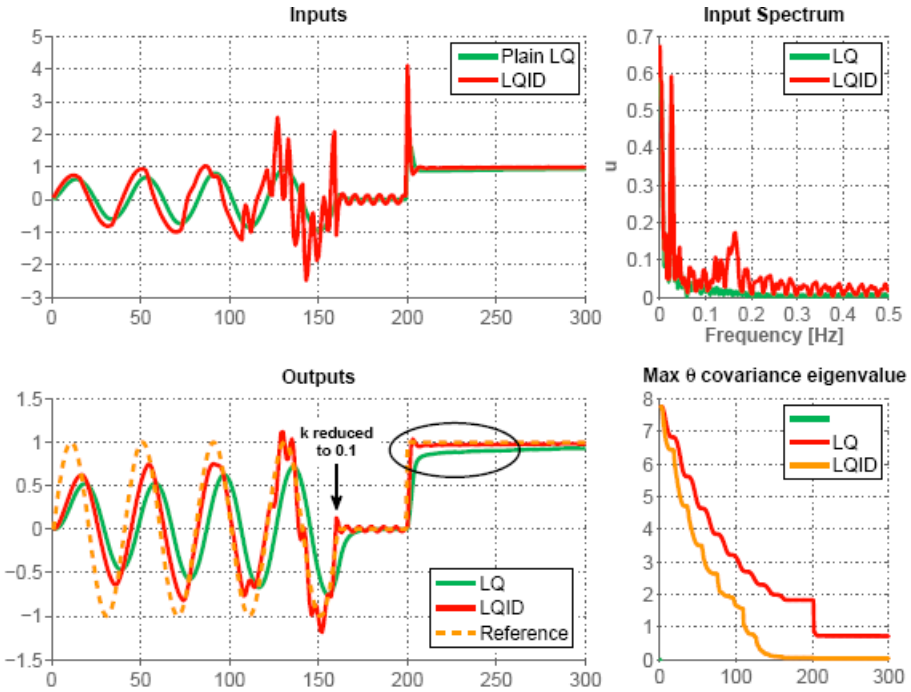

Figure 21 LQID identification compared to LQ. Models are recursively updated in each step.

More details, mathematical formulations and algorithm description can be found in attached publication [HPL4].

2.9 Subspace Identification of Cascade Systems

In Section 2.4, subspace identification for systems with prior information was discussed. In this section, we restrict the attention to systems that has a *cascade structure*, see Figure 1. For this class of systems, it is possible to say more than in the generic case, as seen next.

2.9.1 Introduction

The objective of this section is to study a few methods to identify systems with a cascade, or serial, structure as illustrated in Fig. 1, using subspace methods. The current work has been motivated by a discussion on use of subspace identification in process industry presented in [28].

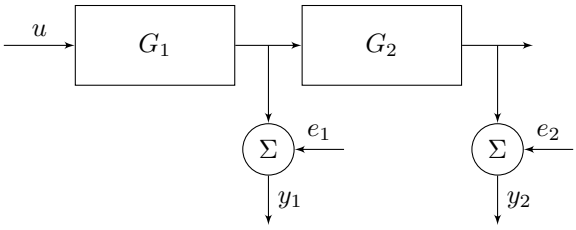

Figure 1: Cascade system.

In particular systems with one input signal and two output signals will be studied. The input-output relations for this system are

$$\begin{array}{rcl} y_1(t) & = & G_1(q)\,u(t) + e_1(t) \\ y_2(t) & = & G_1(q)\,G_2(q)\,u(t) + e_2(t) \end{array} \tag{1}$$

The input signal is denoted $u(t)$ and the outputs, $y_1(t)$ and $y_2(t)$ respectively. The signals $e_1(t)$ and $e_2(t)$ are assumed zero mean white Gaussian measurement noise processes with variances λ_1 and λ_2. The transfer functions $G_1(q)$ and $G_2(q)$ are assumed stable. Here q denotes the standard shift operator, i.e. $q^{-1}u(t) = u(t-1)$. The notation $G_3(q) = G_2(q)\,G_1(q)$ will be used throughout this paper.

The problem is hence to identify the subsystems $G_1(q)$ and $G_2(q)$ from data $\{u(t), y_1(t), y_2(t)\}, t = 1 \ldots N$. Any single-input multiple output method could be used, but it is often not straightforward to impose the cascade model structure.

The contribution here is two new methods that integrate structure into the subspace identification of cascade structured systems. The methods are applied to a real system, the double tank process. The method shows comparable performance with state of the art methods. It is hard to say something about the statistical properties for these methods, however these estimates could be used as initial estimates for a Prediction Error Method (PEM) or the Maximum Likelihood (ML) method.

2.9.2 Other Methods and Related Work

One direct approach to identify the subsystems would be to first identify $G_1(q)$ from data $\{u(t), y_1(t)\}$ and then in a second step identify $G_2(q)$ from data $\{\hat{u}_2(t), y_2(t)\}$, where $\hat{u}_2$ is an estimate of the input to the second subsystem $G_2(q)$. If the model estimate $\hat{G}_1(q)$ is good, one could use $\hat{u}_2 = \hat{G}_1(q)\,u(t)$. If the noise variance is low for the first measurement noise process one could use $\hat{u}_2(t) = y_1(t)$. It is also possible to use an optimal predictor of $u_2(t)$ based on the statistical properties of $e_1(t)$.

It is also possible to apply a Prediction Error Method (PEM) orthe Maximum Likelihood (ML) method to this problem [26]. But because of the product $G_1(q)\,G_2(q)$, simple linear model structures such as OE or ARX are not directly applicable. It can however be shown that structured PEM and structured ML are statistically optimal methods for this problem. The statistical properties of these identified models are analyzed in [29], [30]. The Prediction Error based methods or Maximum Likelihood methods often involve solving non-convex optimization problem. It can therefore be difficult to guarantee that during the optimization the global optimum will be found. A way to solve this is to try to find good initial estimates, hopefully lying in the region of attraction for the global optimum. The two proposed methods here could be a way to find such initial estimates.

The problem of imposing some structure into the subspace method is discussed in Section 2.4, but see also [31] where they try to identify OE and ARMAX models using subspace methods. In [32] and [33] they want to guarantee that the identified model with a subspace method is stable when the true linear system is known to be stable.

Another approach proposed in [34] is to identify the transfer functions G_1 and $G_3 = G_1G_2$ and then obtain an estimate of G_2 by solving the following standard H_∞-model matching problem

$$\hat{G}_2 = \arg \inf_{Q \in RH_\infty} \| \hat{G}_3 - Q\hat{G}_1 \|_\infty \tag{2}$$

where $\hat{G}_1$ and $\hat{G}_3$ are the identified models of G_1 and G_3 respectively. Typically the order of $\hat{G}_2$ is equal to the order of $\hat{G}_1$ plus the order of $\hat{G}_3$. The order of G_2 should be the order of G_3 minus the order of G_1 if there is no pole-zero cancellation. In [34] they solve this by using structured model reduction to reduce the order of G_2.

2.9.3 Subspace Identification of Cascade Systems

In this section some basic properties for cascade systems that are needed for the new identification methods, are presented. The two new methods will be based on subspace identification. A good overview of the algorithm can be found in [27] and [26].

One natural realization of the system (1) on state space form is

$$\begin{aligned} \begin{bmatrix} x_2(t+1) \\ x_1(t+1) \end{bmatrix} &= \begin{bmatrix} A_2 & B_2C_1 \\ 0 & A_1 \end{bmatrix} \begin{bmatrix} x_2(t) \\ x_1(t) \end{bmatrix} + \begin{bmatrix} 0 \\ B_1 \end{bmatrix} u(t) \\ \begin{bmatrix} y_2(t) \\ y_1(t) \end{bmatrix} &= \begin{bmatrix} C_2 & 0 \\ 0 & C_1 \end{bmatrix} \begin{bmatrix} x_2(t) \\ x_1(t) \end{bmatrix} + \begin{bmatrix} e_2(t) \\ e_1(t) \end{bmatrix} \end{aligned} \tag{3}$$

where $x_1(t) \in \mathbb{R}^{n_1}$, $x_2(t) \in \mathbb{R}^{n_2}$ and,

$$G_1(q) = C_1(qI - A_1)^{-1}B_1, \quad G_2(q) = C_2(qI - A_2)^{-1}B_2.$$

This special structure of the state space matrices, where the states $x_1(t)$ correspond to the first subsystem and the states $x_2(t)$ correspond to the second subsystem, will be called a *realization in cascade form*. Note that the matrix B_2C_1 should have $\operatorname{rank}(B_2C_1) = 1$.

Just applying a standard subspace method to the system (1) would return an estimate in the form

$$\begin{aligned} x(t+1) &= Ax(t) + Bu(t) \\ y_1(t) &= C_1x(t) \\ y_2(t) &= C_2x(t) \end{aligned}$$

A state space realization is not unique with respect to the input-output relation, i.e. the system is only identified up to an unknown similarity transform. In general the states from the first subsystem will

be mixed with the states from the second subsystem, due to this unknown transform. The first and second subsystems could hence not be directly separated. If the similarity transform somehow was known, the system could be transformed back to cascade form (3) and the state space matrices for G_1 and G_2 could easily be recovered. In the first proposed method a transform that transforms the system back to cascade form is found and from this the subsystems are recovered.

Basically, the subspace method forms an estimate of the extended observability matrix from input-output data. As discussed before the estimate is a transformed estimate of the true observability matrix. The estimated extended observability matrix, $\tilde{O}_r$, has the form [26]

$$\tilde{O}_r = \begin{bmatrix} C \\ CA \\ \vdots \\ CA^{r-1} \end{bmatrix} \tilde{T} + \tilde{E}_N$$

where $\tilde{T}$ is an unknown transformation of full rank and $\tilde{E}_N$ is an unknown matrix due to noise. The model order is determined by studying the singular values for the extended observability matrix and keep the n most significant values. When the model order has been selected the estimate of $\hat{C}$ and $\hat{A}$ can be calculated from the extended observability matrix by solving a linear least square problem. The matrices $\hat{B}$ and $\hat{D}$ can then be found by solving a linear regression problem. [27], [26].

For the system on cascade form (3) the extended observability matrix becomes

$$\tilde{O}_r\tilde{T} = \begin{bmatrix} C \\ CA \\ \vdots \\ CA^{r-1} \end{bmatrix} \begin{bmatrix} \tilde{T}_{11} & \tilde{T}_{12} \\ \tilde{T}_{21} & \tilde{T}_{22} \end{bmatrix} =$$

$$\begin{bmatrix} C_1\tilde{T}_{11} & C_1\tilde{T}_{12} \\ C_2\tilde{T}_{21} & C_2\tilde{T}_{22} \\ C_1A_1\tilde{T}_{11} & C_1A_1\tilde{T}_{12} \\ \star & C_2B_2C_1T_{12} + C_2A_2\tilde{T}_{22} \\ C_1A_1^2\tilde{T}_{11} & C_1A_1^2\tilde{T}_{12} \\ \star & (C_2B_2C_1A_1 + C_2A_2B_2C_1)\tilde{T}_{12} + C_2A_2^2\tilde{T}_{22} \\ \vdots & \vdots \end{bmatrix} \tag{4}$$

Some repeated values are replaced by stars ($\star$) due to space limitations. This fundamental structure of the extended observability matrix will be used to derive the second method to identify the subsystems.

2.9.4 Identification Methods

The observations made in the previous section are used to formulate two methods for identification of cascade systems.

Method 1: Indirect Method The main idea of this method is to find a similarity transform for the identified system G_3 such that the transformed system is in cascade form (3).

This method of finding a similarity transform that brings the system to cascade form was proposed in [35]. The transformation matrix is parameterized and a set of equations that has to be solved to get the system to cascade form is formulated. It is shown that the number of parameters is less than the number of equations needed to be solved. Due to uncertainties this problem does not in general have an exact solution. In [35] no method of solving this problem is presented. The proposed

method here solves this problem by finding a similarity transform that takes the system to cascade form while minimizing the mean square error between the estimated output and the measured output. The method introduced here is related to the method proposed in [31] where OE and ARMAX models are estimated with subspace methods by finding suitable transformations, to get the system to the desired form. The method denoted method 1 has three steps:

Step 1: Identify the state space matrices $\hat{A}_1$, $\hat{C}_1$, $\hat{B}_1$ from data $\{u(t), y_1(t)\}, t = 1 \dots N$ with order n_1 and $\hat{A}_3$, $\hat{C}_3$ and $\hat{B}_3$ using $\{u(t), y_2(t)\}, t = 1 \dots N$ with order n_3. The order of the second subsystem is calculated as $n_2 = n_3 - n_1$.

Step 2: Find a transformation, T by solving the following optimization problem,

$$\begin{aligned} \min_{T,\tilde{B}_1} \quad & \frac{1}{\lambda_1}\sum_{t=1}^{N}\left(\hat{C}_1\left(qI-\hat{A}_1\right)^{-1}\hat{B}_1 u(t) - y_1(t)\right)^2 + \\ & \frac{1}{\lambda_2}\sum_{t=1}^{N}\left(\hat{C}_3 T\left(qI - T^{-1}\hat{A}_3 T\right)^{-1}\begin{pmatrix}0\\ \tilde{B}_1\end{pmatrix} u(t) - y_2(t)\right)^2 \\ \text{s.t} \quad & T^{-1}\hat{A}_3 T \text{ and } \hat{C}_3 T \text{ are in cascade form.} \end{aligned} \tag{5}$$

where λ_1 and λ_2 are the measurement noise variances or can be seen as some weighting if the variances are unknown.

The D-matrices are assumed zero here but an extension to non-zero D-matrices should be easy. Some of the constraints should be chosen such that the lower right corner of $T^{-1}\hat{A}_3 T$ has approximately the same dynamics as the identified system $\hat{G}_1$ and that the lower left corner should contain zeros. The upper right corner of $T^{-1}\hat{A}_3 T$ corresponding to $B_2 C_1$ should have rank 1. It is not obvious how these constraints should be chosen when the first subsystem has a order larger than one. Hence the optimization problem stated above is in general hard to solve.

Let us study the constraints in more detail. First look at the constraint that $\hat{C}_3 T$ should be on cascade form. This means that the last n_1 elements of $\hat{C}_3 T$ should be equal to zero. This in turns means that the last n_1 columns of T must be in the kernel space of $\hat{C}_3$. The second set of constraints is that $T^{-1}\hat{A}_3 T$ should be on cascade form. This means that the lower right corner should have similar dynamics as the first identified subsystem $\hat{G}_1$ and that the lower left corner should be the zero matrix.

If we use Schur factorization[36] on $\hat{A}_3$

$$\hat{A}_3 = U\tilde{A}_3 U^* \tag{6}$$

then $\tilde{A}_3$ is similar to $\hat{A}_3$ and has the lower left corner equal to the zero matrix. If the Schur factorization is performed such that the eigenvalues closest to the eigenvalues of the first subsystem is located in the lower right corner of $\tilde{A}_3$, the first n_2 columns of T should be chosen as the first columns of U. This is summarized in a proposition.

Proposition 1 *If the last n_1 columns in T spans the kernel space of C_3 and the first n_2 columns span the space corresponding to the n_2 columns of U, where U is given from the Schur factorization of $A_3 = U\tilde{A}_3 U^*$ such that the dynamics from the first system is in the lower right corner of the block-triangular matrix $\tilde{A}_3$. The system transformed with T will be on cascade form.*

Using Proposition 1, the optimization problem (5) could be simplified. If the optimization is instead performed over linear combinations of the vectors spanning the kernel space of C_3 and over scaled versions of the appropriate columns of U from the Schur factorization. Denoting the order of the kernel space by $n_K = n_2 + n_1 - 1$ gives

$$T = [k_1 u_1 \dots k_{n_2} u_{n_2}, \sum_{i=1}^{n_K} k_{i+n_2} c_i \dots \sum_{i=1}^{n_K} k_{i+n_2+(n_1-1)n_K} c_i] \tag{7}$$

where u_i is the i:th column of U from the Schur factorization (6) and $c_i \in \mathrm{Ker}(\hat{C}_3)$. The optimization is performed over k_i $i = 1 \ldots (n_2 + n_1(n_2 + n_1 - 1))$. The number of optimization parameters are reduced from $(n_1 + n_2)^2$.

Finally, the constraint that the rank of the upper right corner of $T^{-1}\hat{A}_3 T$, denoted $\hat{A}_{12}$, should be one is hard to incorporate. Instead some heuristics could be used. Here we will use that the upper right corner should equal $B_2 C_1$. Denote the estimate of the system matrix of the first subsystem from $T^{-1}\hat{A}_3 T$ as $\bar{A}_1$. We denote $\bar{C}_1(T)$ as the transformed matrix of $\hat{C}_1$ where the transform is a similarity transform between the identified $\hat{A}_1$ and $\bar{A}_1$. Ideally the eigenvalues of $\hat{A}_1$ should be the same as the eigenvalues $\bar{A}_1$. If this is the case a similarity transform could easily be found. In general this is not the case. One solution to this is to transform both $\hat{A}_1$ and $\bar{A}_1$ to upper triangular form, then replace the eigenvalues in the diagonal of $\bar{A}_1$ by the corresponding in $\hat{A}_1$. This way the two matrices are similar and a similarity transform could be found. An estimate of B_2 is then given by

$$\hat{B}_2 = \hat{A}_{12}\bar{C}_1(T)^{\dagger}$$

where $(\dagger)$ denotes the pseudo inverse. We now formulate the following optimization problem

$$\begin{aligned} \min_{T,\tilde{B}_1} \quad & \frac{1}{\lambda_1}\sum_{t=1}^{N}\left(\hat{C}_1\left(qI - \hat{A}_1 T\right)^{-1}\tilde{B}_1 u(t) - y_1(t)\right)^2 + \\ & \frac{1}{\lambda_2}\sum_{t=1}^{N}\left(\hat{C}_2\left(qI - \hat{A}_2\right)^{-1}\hat{B}_2\hat{C}_1\left(qI - \hat{A}_1 T\right)^{-1} u(t) - y_2(t)\right)^2 \end{aligned} \tag{8}$$

where

$$\begin{aligned} \hat{C}_2 &= (CT)_{1:n_2} \\ \hat{B}_2 &= \hat{A}_{12}\bar{C}_1^{\dagger} \\ \hat{A}_2 &= \left(T^{-1}\hat{A}_3 T\right)_{1:n_2,1:n_2}. \end{aligned}$$

The optimization is performed over columns of T defined in (7) and $\tilde{B}_1$. This heuristics solves the problem with the rank condition in many cases.

Step 3: When the transformation is found the system is transformed to cascade form. From this the estimates of the state space matrices for the second subsystem $\hat{A}_2$ and $\hat{C}_2$ can easily be recovered. The matrix estimate $\hat{B}_2$ could be calculated from the matrix product $B_2 C_1$ as described above.

Method 2: Direct Method The second method uses the fact that the structure of the extended observability matrix is known for cascade systems, see (4). The method only works for systems where both subsystems have order one. But this is in practice a common case.

The method consists of the following steps:

Step 1: Identify the first subsystem using data u and y_1 with order n_1.

Step 2: Identify the extended observability matrix for the Single-Input Multiple-Output (SIMO) system from u to y_1 and y_2 with order n_3. Denote the identified extended observability matrix

$$O_r\tilde{T} = \begin{bmatrix} \xi_{1,1} & \xi_{1,2} \\ \eta_{1,1} & \eta_{1,2} \\ \vdots & \vdots \\ \xi_{r,1} & \xi_{r,2} \\ \eta_{r,1} & \eta_{r,2} \end{bmatrix}$$

where $\xi_{i,1}$ has size $(1 \times n_1)$ and $\eta_{i,2}$ has size $(1 \times n_3 - n_1)$.

Step 3: From (4) it can be seen that for the first subsystem the state space matrices can be solved with least squares just as in the standard subspace formulation

$$\hat{C}_1 = C_1\tilde{T}_{11} = \xi_{1,1}$$

$$\hat{A}_1 = \arg\min_{A_1} \sum_{i=1}^{r-1} \left\| \xi_{i+1,1} - \xi_{i,1}A_1 \right\|_2^2$$

Step 4: From (4) it is seen that for the second subsystem the estimate $\hat{C}_2$ is given by

$$\hat{C}_2 = C_2\tilde{T}_{22} = \eta_{1,2}$$

In general it is not obvious how a a least square problem should be formulated for the second subsystem. To illustrate the concept we consider the special case when the order of the second subsystem is one. Denoting the matrix product $\chi = B_2C_1$ gives the following least square problem in $\hat{A}_2$ and χ.

$$\arg\min_{A_2,\chi} \sum_{i=1}^{r-1} \left\| \eta_{i+1,2} - \eta_{i,1}A_2 - \chi\xi_{i,2} \right\|_2^2$$

Step 5: When $\chi = B_2C_1$ has been found, $\hat{B}_2$ can be solved. Finally $\hat{B}_1$ can be calculated as in the standard subspace formulation as a linear regression problem.

2.9.5 Examples

In this section the two methods presented will first be applied to a real application, the double tank process, and then the first direct method will be applied to a simulated system to show how the method performs for higher order systems.

The Double Tank Process The double tank system from *Quanser Inc* consists of two equivalent water tanks. A DC-motor drives a pump which pumps water from the basin into the upper tank. Water then flows out from the upper tank into the lower tank through a small outlet. The water from the lower tank then flows out into the basin. The input to the system is the input voltage to the DC-motor, u and the outputs are the water level in each tank, h_1 and h_2.

The process is nonlinear. The outflow from one tank is proportional to the square root of the water level. The identification of the system will hence be performed around a linearization point.

Identification A white Gaussian noise process is used as input during the identification. The sampling time is chosen as $T_s = 1s$. 300 samples of the input and outputs were collected, 200 used for identification and 100 used for validation. When all data has been collected, the identification process starts. The methods presented in section 2.9.4 are used and their results are compared. First Method 1 is considered.

Method 1 The state space matrices, $\hat{A}_1$, $\hat{B}_1$, $\hat{C}_1$, $\hat{A}_3$ and $\hat{C}_3$ are identified with *N4SID* [26], [27]. The orders of these systems are chosen by looking at the singular values of their respective extended observability matrices.

The order of G_1 is chosen as $n_1 = 1$ and the order for G_3 is chosen as $n_3 = 2$.

A similarity transform is found by solving the optimization problem (8) numerically. Since the orders of the subsystems are both one, the rank condition is automatically fulfilled. When the transformation matrix T and $\tilde{B}_1$ are found then it is straightforward to find $\hat{A}_2$, $\hat{B}_2$ and $\hat{C}_2$.

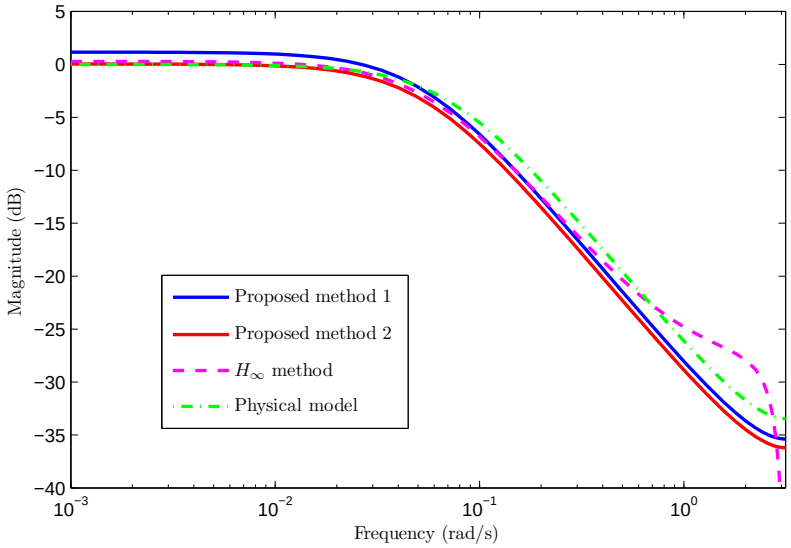

Figure 2: Bode magnitude plot of the second subsystem G_2 for the two proposed method, the physical model and the H_∞-method.

Method 2 Again the *N4SID* is used, but now on the SIMO system to get an estimate of the extended observability matrix. The singular values of the extended observability matrix suggest that the order should be chosen as 2. From previous results we know that the first subsystem is approximated well by a first order system. Method 2 is now applied to the extended observability matrix and the state space matrices for the two subsystems are calculated.

Results The methods previous applied to the two tank process are compared to a physical model [37] and the H_∞-method (2), [34].

For the first subsystem the two proposed methods and the H_∞-method gives similar result. This is obvious since all three methods are estimating the first subsystem in the same way. They also have about the same dynamics as the physical model and only a very small difference in gain. The difference in gain could originate from wear and tear in the real process as well as from the discretization and linearization in the physical model.

The bode plot for the second system for the two different methods are shown in Fig. 2. For the second subsystem the methods gives slightly different results. First we can note that the estimated system using the H_∞-method is of order 3 as expected. The dynamics are about the same for the two proposed methods, i.e. the eigenvalues of system matrix are close but they differ from the H_∞-method. As the two tanks are equal we would expect the dynamics of the first and second subsystem to be equal. This can be seen in the physical model. This is the case in both of the proposed methods but not in the H_∞-method.

The gain difference, that can be seen between the two proposed methods, is due to the different way the two methods calculates the state space matrices.

Finally the prediction error for the models given by the three methods, are calculated for the validation data, i.e.

$$V\left(\hat{G}_1, \hat{G}_2\right) = \frac{1}{N}\sum_{t=1}^{N}\left(y_1(t) - \hat{G}_1(q)\,u(t)\right)^2 + \left(y_2(t) - \hat{G}_1(q)\,\hat{G}_2(q)\,u(t)\right)^2 \tag{9}$$

The resulting prediction error is $4.2 \cdot 10^{-4}$ for the indirect method, $3.8 \cdot 10^{-4}$ for the direct method and

$3.9 \cdot 10^{-4}$ for the H_∞-method. The difference in prediction errors for the three methods is small.

It looks like the second method performs slightly better for this simple system. The execution time is also much shorter for this method since the optimization, i.e. the solving of the least square problem, is much more computational efficient than for the first method. But on the other hand, it is not obvious how the second method should be extended to handle larger systems.

Higher order systems Here we consider a numerical example of a cascade system with higher order subsystems

$$G_1(q) = \frac{q - 0.1}{(q + 0.6)(q - 0.8)}$$
$$G_2(q) = \frac{1}{(q^2 - 0.5q + 0.5)}$$

The measurement noise variances are $\lambda_1 = 1$ and $\lambda_2 = 1$. The input is white Gaussian noise with unit variance. The system is simulated for 500 data points and the indirect method is then applied, this is repeated 100 times. The result of the Monte-Carlo simulation is shown for the second subsystem in Fig. 3. The first subsystem is the same as for direct application of the standard subspace method.

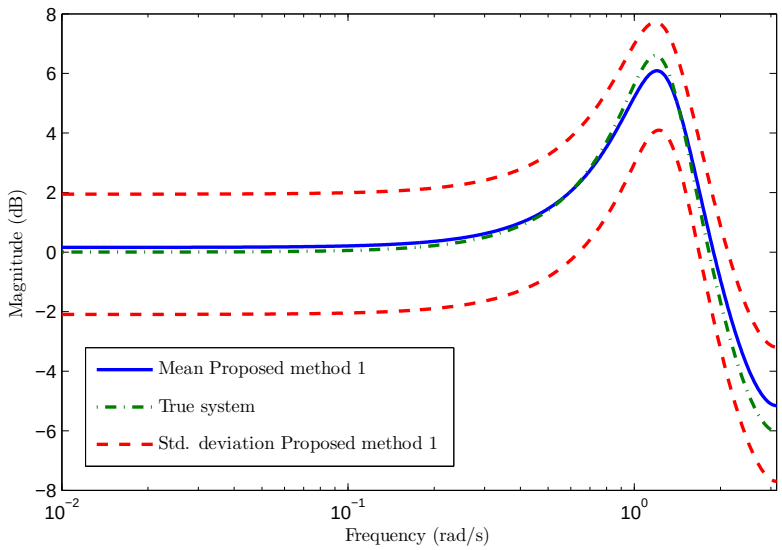

Figure 3: The mean and standard deviation of the Monte-Carlo simulation for the second subsystem.

From the figure it can be seen that the method performs well for this system. It seems that the mean over the Monte-Carlo simulations tends to the true system. The prediction error (9) is comparable with the direct subspace method applied to the SIMO system from u to y_1 and y_2.

2.10 Input Design for Cascade Systems

In Section 2.8, optimal experiment design is discussed for generic model structures. Here we again restrict the model structure to a cascade form, and see what implications that have for an optimal experiment.

In the identification of the double tank system in Section 2.9.5, the input was chosen as a Gaussian white noise sequence. This it not generally the optimal input for the identification of a cascade system. The problem is that the input to the second system can not be chosen directly. We consider the input signal to the second subsystem

$$u_2(t) = G_1(q)u(t)$$

which consequently is directly colored by the the first unknown subsystem. Hence, a good input for identification of G_1 may give a bad input to G_2 and vice versa.

The recent framework [38] for experiment design, introduced by Hjalmarsson and co-workers could be interesting to apply to cascade systems. The main idea of this framework is that the estimation properties could be separated from the application specification.

To illustrate the framework an example is given for a simple cascade system. Consider the cascade system with first order FIR subsystems, i.e. $G_1(q) = 1 + b_1 q^{-1}$ and $G_2(q) = 1 + b_2 q^{-1}$. The model parameter vector is denoted $\theta = \begin{bmatrix} b_1 & b_2 \end{bmatrix}$ and assume that the true system can be described by $\theta_0 = \begin{bmatrix} b_1^0 & b_2^0 \end{bmatrix}$.

Assume that we have some requirements on the parameter covariance, then the application specification could be written as

$$V_{\text{app}}(\theta) = \begin{bmatrix} b_1 - b_1^0 & b_2 - b_2^0 \end{bmatrix} Q \begin{bmatrix} b_1 - b_1^0 \\ b_2 - b_2^0 \end{bmatrix} \leq \frac{1}{\gamma}$$

where Q is some weighting matrix and $\gamma > 0$ is some constant . This weighting matrix could for example be chosen such that the parameter in the second subsystem is more important than the parameter for the first subsystem or vice versa.

Now consider a typical system identification method that minimizes the mean square prediction error, i.e.

$$\begin{aligned} \hat{\theta}_N &= \arg\min_{\theta} V_{ID,N}(\theta) \\ V_{ID,N}(\theta) &= \frac{1}{N}\sum_{t=1}^{N} \frac{\left(y_1(t) - \left(1 + b_1 q^{-1}\right) u(t)\right)^2}{\lambda_1} + \\ &\quad \frac{1}{N}\sum_{t=1}^{N} \frac{\left(y_2(t) - \left(1 + b_1 q^{-1}\right)\left(1 + b_2 q^{-1}\right) u(t)\right)^2}{\lambda_2} \end{aligned}$$

We will now try to find the optimal input for this problem. The input should be optimal in the sense that it minimizes the input power such that the application specifications are fulfilled. This is known as least costly identification [39]. Using the framework [38], asymptotically ($N \to \infty$) it can be shown that this optimization problem can be formulated as

$$\begin{aligned} \min_{u(t)} \quad & E\left[u(t)^2\right] \\ \text{s.t} \quad & \gamma V''_{\text{app}} \leq N V''_{\text{ID}} \end{aligned}$$

where the constraint is a matrix inequality.

For the simple system presented above the optimization problem becomes

$$\begin{aligned} \min_{r_0} \quad & r_0 \\ \text{s.t} \quad & N \begin{bmatrix} \rho_1 & \rho_2 \\ \rho_2 & \rho_3 \end{bmatrix} \geq \gamma Q \\ & r_0 \geq r_1 \end{aligned}$$

$$\begin{aligned} \rho_1 &= r_0/\lambda_1 + [(1 + b_2^2) r_0 + 2 b_2 r_1]/\lambda_2 \\ \rho_2 &= [(1 + b_1^2) r_0 + 2 b_1 r_1]/\lambda_2 \\ \rho_3 &= [(1 + b_1 b_2) r_0 + (b_1 + b_2) r_1]/\lambda_2 \end{aligned}$$

where $r_\tau = \bar{E}\left[u\left(t\right)u\left(t-\tau\right)\right]$. The optimization problem is solved for r_0 and r_1 and a optimal input with this covariance function could be generated.

Let us look at some special cases. First assume that $\lambda_2 \gg \lambda_1$ and that the parameter b_2 is unimportant. Then we get $r_1 = 0$, i.e. the input should be chosen as white noise as expected, we know that this is a optimal input for the MA(1) process. If we instead consider $\lambda_1 \gg \lambda_2$ and that the first parameter, b_1 is unimportant, then we would want a white noise input to the second subsystem. If the optimization problem above is solved the input becomes a white noise sequence filtered through the inverse of the first subsystem, hence the input to the second becomes white noise.

In general the input becomes an optimal weighting between these two cases depending on the noise levels and which parameter that is more important.

For more complex systems, the problem above cannot be solved for the covariance function r_τ but the optimization problem must be solved for a parametrization of the spectrum of $u\left(t\right)$, see [38]. It would be interesting to study the optimal input for more complex systems.

2.11 MPC oriented system identification

Applications oriented system identification is a research topic that has attracted significant interest since the birth of the field system identification in the mid 1960s. In particular there was a surge of interest in conjunction with the developments in robust control between 1985-1995, giving rise to the area "identification for control" [1, 2, 3, 4, 5, 6, 7, 8, 9, 10, 11, 12, 13, 14]. A key outcome of this effort was the recognition of the importance of the experiment design[1] and this lead to iterative approaches trying to achieve experimental conditions such that the bias error was suitably distributed over frequencies to suit control applications.

A consequence of these developments was that results on computational methods for optimal experiment design were revisited and extended [15, 16, 17, 18, 19].

In [20] it is illustrated that optimal input design may result in significant savings in experimental efforts in control applications. Through some simple examples, it was advocated in [21] that it is possible to combat the curse of complexity, i.e. that the model uncertainty grows with the system complexity so that for highly complex systems the model becomes virtually useless, by careful experiment design and that this also allows simple models to be used (as long as only a limited amount of system properties are to be extracted from the measurements). Following up on [21], the dual role of a "good" input as 1) an enhancer of system properties of interest, and 2) as an attenuator of properties of little or no interest was formalized in [22] and further developed in [23]. In particular it was shown that, under certain conditions, an input that is designed to be optimal for a scalar cost function and for a full order model, results in experimental data for which also reduced order models can be used to consistently identify the property of interest.

In [KTH1, KTH3] it is argued that the main resource to cope with system complexity is the experiment design and a a general framework for applications oriented experiment design is outlined.

In summary, applications oriented system identification has turned out to be a very complex issue with many facets and there is to date no entirely satifying general methodology even though many of the important characteristics of the problem are well recognized. Due to the recognition of the profound importance of experiment design, the WIDE research group at KTH has pursued this research direction. The limitations in resources for Task 3.1 has imposed limitations on what the Lab has been able to achieve. The focus has been to develop a framework for experiment design for (distributed) MPC and to test the principles. When assessing the contributions, the large efforts that has been spent on applications system identification by the research community should be considered. Over-

[1] This, of course, was well known earlier on also but during this time its importance became very palpable.

all, we believe that the results are very promising, but that some further developments are needed in order to be practically useful.

2.11.1 Basic ideas

The quality of a model will directly influence the performance of an application where the model is being used. We assume that if an exact mathematical model of the true system was available for the design of the application, the desired performance would be obtained. However, when the used model does not correspond to the true system, the performance of the application will degrade. We measure this in terms of a performance degradation "cost" $V_{app}(M)$ which has global minimum $V_{app}(M) = 0$ at $M = \mathcal{S}_o$, c.f. [24, 25]. For example, in MPC the performance degradation can be measured by

$$V_{app}(M) := \sum_{t=1}^{N} \|y_{ideal}(t) - y_M(t)\|^2 \tag{10}$$

where y_{ideal} is the output response when the true system model is used in the MPC and where y_M is the response when model M is used instead.

A model is then deemed to be acceptable if its performance degradation is sufficiently small. This leads to a set of acceptable models

$$\mathcal{E}_{app} := \left\{ M : V_{app}(M) \leq \frac{1}{\gamma} \right\} \tag{11}$$

Here γ is a user specified constant that determines the required accuracy. We will call this constant, the desired accuracy since increasing γ leads to tighter specifications (and hence a smaller set $\mathcal{E}_{app}$.

This leads to the simple idea that the objective of applications oriented system identification is to produce a model which belongs to $\mathcal{E}_{app}$.

In WIDE a stochastic framework is adopted in that disturbances are assumed to be random variables. Resulting parameter estimates (which corresponds to models) will then also be random variables, typically with unbounded support, and as a consequence it is not possible to to provide 100% guarantee that the resulting model belongs to $\mathcal{E}_{app}$. Instead, this has to be relaxed to a certain level of probability, e.g. 99%.

For parameter identification, the model parameters, say θ, correspond to the models $M(\theta)$ and the objective is then that the parameter estimate, $\hat{\theta}$ say, belongs to the set of model parameters that corresponds to $\mathcal{E}_{app}$ with a certain (high) level of probability p, i.e.

$$\text{Probability}\left(\left\{ \hat{\theta} : M(\hat{\theta}) \in \mathcal{E}_{app} \right\} \right) \geq p \tag{12}$$

2.11.2 Applications oriented experiment design

One thus has to ensure that the experiment design is such that (12) holds. A natural objective is to try to minimize the experimental resources required to ensure this. Resources could, e.g., mean experimental time or used energy. Thus the experiment design problem in applications oriented parameteric system identification can be formulated as follows

$$\begin{aligned} &\min \text{Experimental Resources} \\ &\text{s.t. Probability}\left(\left\{ \hat{\theta} : M(\hat{\theta}) \in \mathcal{E}_{app} \right\} \right) \geq p \end{aligned} \tag{13}$$

There two several key issues associated with solving this problem in practice:

i) The set of acceptable models $\mathcal{E}_{app}$ has to be determined

ii) It must be, at least, numerically possible to solve the problem (13)

2.11.3 MPC oriented experiment design

In regards to the issues in the preceeding section, two methods to compute $\mathcal{E}_{app}$ for MPC are detailed in [KTH8, KTH5]. In the next section we describe the scenario approach employed in [KTH8]. A hampering factor is that the system parameters need to be known. An adaptive method to cope with this is presented in [KTH2] for ARX systems but this method still has to be adapted to MPC. For ii) in Section 2.11.2, we are relying on results in [19] where it is shown that optimal experiment design problems can be solved by convex optimization when the system is linear and time-invariant if the input spectrum is linearly parameterized.

2.11.4 The Scenario Approach

Consider the following general Robust Convex Program:

$$RCP: \quad \begin{array}{ll} \min\limits_{\gamma\in\mathbb{R}^d} & c^T\gamma \\ \text{s.t.} & f_\delta(\gamma)\leq 0, \quad \delta\in\Delta. \end{array} \tag{14}$$

where $f_\delta : \mathbb{R}^d \to \mathbb{R}$ is convex for every $\delta \in \Delta$.

The description of RCP involves the satisfaction of an infinite number of constraints, i.e., one per each value of $\delta \in \Delta$. This corresponds to a convex optimization problem which, except for some particular cases, is in general computationally intractable.

The scenario approach, see [40], provides a tractable relaxation of RCP, which consists in selecting a small number of these constraints to include in the optimization problem. To do this, the scenario approach presumes a probabilistic description of the uncertainty, in other words, a probability distribution P_r over Δ. The method then extracts, at random, N instances or 'scenarios' of the uncertainty parameter δ according to the probability P_r, and it considers only the corresponding constraints in the scenario optimization problem.

The resulting program, SCP_N, is a standard finite dimensional convex optimization problem with a finite number of constraints. The computational cost of SCP_N can be quite reasonable, provided N is not large.

2.11.5 Optimal input design for MPC

Consider prediction error identification of models of the type

$$x(t+1) = A(\theta)x(t) + Bu(t) \tag{15}$$

$$y(t) = x(t) + e(t), \tag{16}$$

where the state transition matrix is parameterized by θ. The resulting parameter estimates are asymptotically Gaussian with covariance matrix P. The inverse P^{-1} is a linear function of the input spectral density and a linearly parameterized spectrum gives a convex optimization problem.

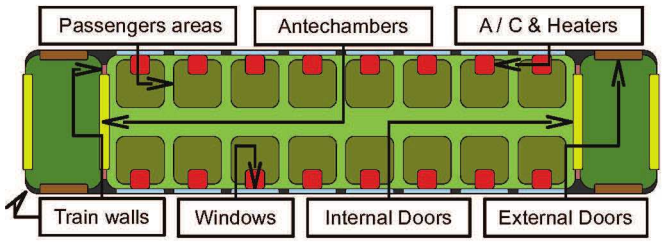

Figure 4: Layout of the railcar as presented in [44]

We study the input design problem

$$\min_{\Phi_u(\omega)} \quad \mathrm{tr} \int_{-\pi}^{\pi} \Phi_u(\omega) \tag{17}$$

$$\text{s.t.} \quad (\theta_0 - \theta)^T \frac{N}{\kappa} P^{-1} (\theta_0 - \theta) \geq \gamma V_{app}(\theta) \tag{18}$$

$$\Phi_u \geq 0, \quad \forall \omega. \tag{19}$$

In the inequality (18) the left side corresponds to a confidence ellipsoid of the parameter estimates while the right side corresponds to the estimates falling in the set $\mathcal{E}_{app}$. This implies that we guarantee that the estimates with a certain probability will give an acceptable degradation (10) of the MPC performance. No analytic description of V_{app} is used, instead the ideas from the scenario approach are used to satisfy the constraints.

One advantage of MPC is the ability to easily handle constrained input and output signals in the controller. A short-coming of the current method is that hard constraints are not taken into account in the input design.

2.11.6 The railcar example

We will consider identifying a model of a railcar that is to be used for temperature control by MPC found in [44]. The layout of the railcar is presented in Figure 4. We model the interactions in the railcar using the heat conduction equation and the model of the railcar is

$$T(t+1) = A(\theta)T(t) + Bu(t) \tag{20}$$

$$y(t) = T(t) + e(t) \tag{21}$$

where T is the temperatures in the compartments and A is parameterized by θ. The model has in total 18 states, 8 inputs and 18 outputs. More details of the model and the MPC problem can be found in [44] while the input design problem considered is described in detail in [KTH8].

Optimal inputs spectral densities for minimizing the total input energy while maintaining an acceptable application degradation are found for different types of spectrum. We see that allowing spatial and temporal coloring reduces the amount of input energy needed. Figure 5 shows three FIR-type optimal spectral densities, only the upper left 4×4 block in shown since the symmetry of the railcar gives identical blocks in the spectrum. The total input energy for the different design is presented in Table 1. We also note that the input energy in the corner compartments in all designs is the highest, this is reasonable since there is no actuation in the ante chambers.

2.11.7 Summary

In summary, one part of the WIDE approach to MPC oriented system identification is to focus on the experiment design. The objective is to minimize use of experimental resources, while ensur-

Table 1: The total input power required to achieve the identification goal for four different types of input spectra. For the FIR spectra, M denotes the maximum time delay in the filter. All other parameters of the optimization are kept the same in all four experiments.

	Spectrum type			
	White	FIR, M = 0	FIR, M = 1	FIR, M = 2
Input Power	225	150	114	102

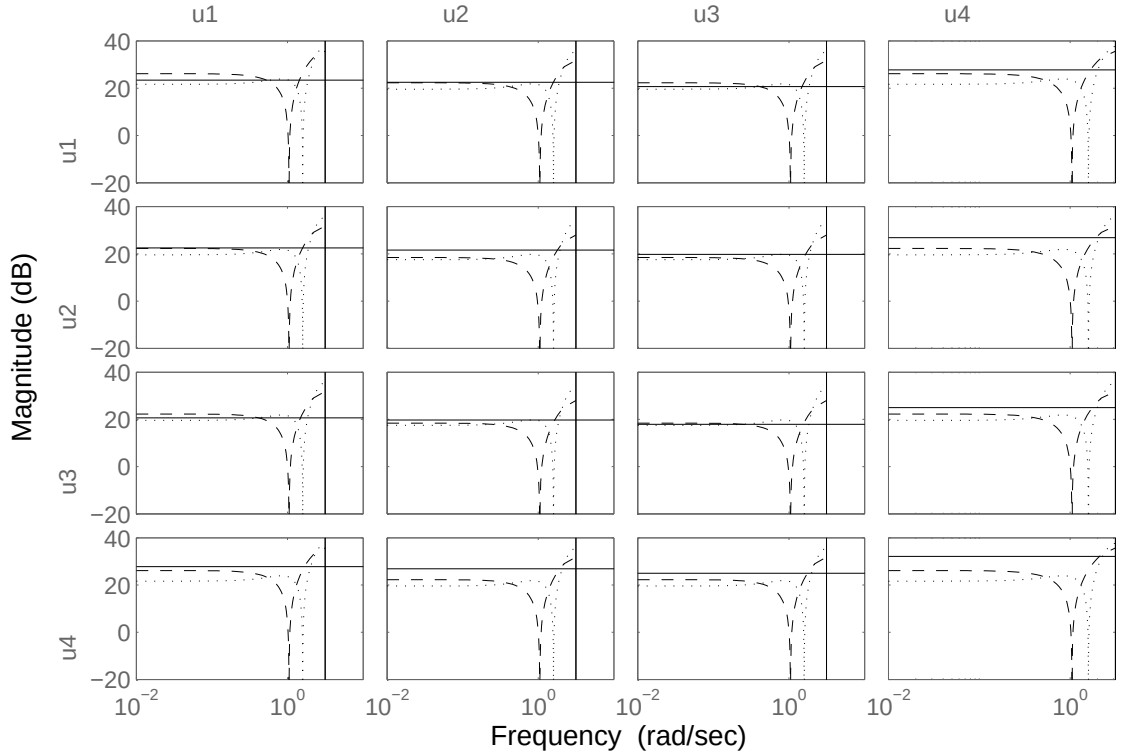

Figure 5: The upper left 4×4 block of the optimal input spectrum for identification of the railcar model parameters with different spectrum parameterization, $M = 0$ (solid), $M = 1$ (dashed), $M = 2$ (dotted).

ing that the requirements of the MPC application are satisfied. The solution is obtained by convex optimization. For further details we refer to [KTH8, KTH5, KTH1, KTH3].

.

Bibliography

[1] M. Gevers. Connecting identification and robust control: A new challenge. In *Proc. IFAC/IFORS Symposium on Identification and System Parameter Estimation*, Budapest, Hugary, 1991.

[2] R. J. P. Schrama. Accurate models for control design: the necessity of an iterative scheme. *IEEE Transactions on Automatic Control*, 37(7):991–994, 1992.

[3] G.C. Goodwin, M. Gevers, and B. Ninness. Quantifying the error in estimated transfer functions with application to model order selection. *IEEE Trans. Automatic Control*, 37(7):913–928, 1992.

[4] M. Gevers. Towards a joint design of identification and control? In H. L. Trentelman and J. C. Willems, editors, *Essays on Control: Perspectives in the Theory and its Applications*. Birkhäuser, 1993.

[5] D.S. Bayard, Y. Yam, and E. Mettler. A criterion for joint optimization of identification and robust control. *IEEE Trans. Automatic Control*, 37:986–991, 1992.

[6] E.W. Jacobsen. Identification for control of strongly interactive plants. In *Proceedings AIChE Annual Meeting*, San Fransico, California, USA, 1994. Paper 226ah.

[7] Z. Zang, R. R. Bitmead, and M. Gevers. Iterative weighted least-squares identification and weighted LQG control design. *Automatica*, 31(11):1577–1594, 1995.

[8] P.M.J. Van den Hof and R.J.P. Schrama. Identification and control – closed loop issues. *Automatica*, 31(12):1751–1770, 1995.

[9] R.A. de Callafon and P.M.J. Van den Hof. Connecting system identification and robust control by a factorization approach. In *11th IFAC Symposium on System Identification*, volume 1, pages 117–122, Fukuoka, Japan, 1997.

[10] J.M. Böling and P.M. Mäkilä. On control relevant criteria in H_∞ identification. *IEEE Transactions on Automatic Control*, 43(5):694–700, 1998.

[11] G.C. Goodwin. Identification and robust control: Bridging the gap. In *Proceedings 7th IEEE Mediterranean Conference on Control and Automation*, Haifa, Israel, 1999.

[12] D.E. Rivera and K.S. Jun. An integrated identification and control design methodology for multivariable process system applications. *IEEE Control Systems Magazine*, 20(3):25–37, 2000.

[13] S. Malan, M. Milanese, D. Regruto, and M. Taragna. Robust control from data via uncertainty model sets identification. In *Proceedings 40th IEEE Conference on Decision and Control*, Orlando, Florida, USA, December 2001. IEEE.

[14] S.A. Eker and M. Nikolaou. Linear control of nonlinear systems: Interplay between nonlinearity and feedback. *AIChE Journal*, 48(9):1957–1980, 2002.

[15] K. Lindqvist and H. Hjalmarsson. Optimal input design using linear matrix inequalities. In *Proceedings of the 12th IFAC Symposium on System Identification*, 2000.

[16] K. Lindqvist and H. Hjalmarsson. Identification for control: Adaptive input design using convex optimization. In *Conference on Decision and Control*, pages 4326–4331, Orlando, Florida, USA, December 2001. IEEE.

[17] R. Hildebrand and M. Gevers. Identification for control: Optimal input design with respect to a worst-case ν-gap cost function. *SIAM J. Control Optim*, 41(5):1586–1608, 2003.

[18] H. Jansson and H. Hjalmarsson. Mixed $\mathcal{H}_\infty$ and $\mathcal{H}_2$ input design. In *IEEE Conference on Decision and Control*, Bahamas, December 2004.

[19] H. Jansson and H. Hjalmarsson. Input design via LMIs admitting frequency-wise model specifications in confidence regions. *IEEE Transactions on Automatic Control*, 50(10):1534–1549, 2005.

[20] M. Barenthin, H. Jansson, and H. Hjalmarsson. Applications of mixed $\mathcal{H}_\infty$ and $\mathcal{H}_2$ input design in identification. In *16th World Congress on Automatic Control*, Prague, Czech Republik, 2005. IFAC. Paper Tu-A13-TO/1.

[21] H. Hjalmarsson. From experiment design to closed loop control. *Automatica*, 41(3):393–438, March 2005.

[22] H. Hjalmarsson, J. Mårtensson, and B. Wahlberg. On some robustness issues in input design. In *14th IFAC Symposium on System Identification*, Newcastle, Australia, March 2006.

[23] Jonas Mårtensson. *Geometric Analysis of Stochastic Model Errors in System Identification*. PhD thesis, Automatic Control, Electrical Engineering, Royal Institute of Technology (KTH), Stockholm, Sweden, 2007.

[24] M. Gevers and L. Ljung. Optimal experiment designs with respect to the intended model application. *Automatica*, 22(5):543–554, 1986.

[25] U. Forssell and L. Ljung. Some results on optimal experiment design. *Automatica*, 36(5):749–756, May 2000.

[26] L. Ljung. *System Identification: Theory for the User*. Prentice-Hall, Englewood Cliffs, NJ, 2nd edition edition, 1999.

[27] P. van Overschee and B. DeMoor. *Subspace Identification of Linear Systems: Theory, Implementation, Applications*. Kluwer, 1996.

[28] Bo Wahlberg, Magnus Jansson, Ted Matsko, and Mats Molander. *Experiences from Subspace System Identification - Comments from Process Industry Users and Researchers*, pages 315–327. Springer, October 2007.

[29] B. Wahlberg, H. Hjalmarsson, and J. Mrtensson. Variance analysis for identification of cascade systems. In *Decision and Control, 2008. CDC 2008. 47th IEEE Conference on*, pages 131–136, Dec. 2008.

[30] B. Wahlberg, H. Hjalmarsson, and J. Mårtensson. Variance results for identification of cascade systems. *Automatica*, 45(6):1443–1448, 2009.

[31] Christian Lyzell, Martin Enqvist, and Lennart Ljung. Handling certain structure information in subspace identification. In *Proceedings of the 15th IFAC Symposium on System Identification*, April 2009.

[32] T. Van Gestel, J.A.K. Suykens, P. Van Dooren, and B. De Moor. Identification of stable models in subspace identification by using regularization. *Automatic Control, IEEE Transactions on*, 46(9):1416 –1420, sep 2001.

[33] S.L. Lacy and D.S. Bernstein. Identification of FIR wiener systems with unkoiwn, non-invertible, polynomial non-linearities. *International Journal of Control*, 76(15):1500–1507, 2003.

[34] Bo Wahlberg and Henrik Sandberg. Cascade structural model approximation of identified state space model. In *Proceedings IEEE Conference on Decision and Control*, Cancun, Mexico, December 2008.

[35] Bo Wahlberg, Håkan Hjalmarsson, and Jonas Mårtensson. On identification of cascade systems. In *17th IFAC World Congress*, pages 5036–5040, July 2008.

[36] Roger A. Horn and Charles R. Johnson. *Matrix Analysis*. Cambridge University Press, 1990.

[37] K.H. Johansson, A. Horch, O. Wijk, and A. Hansson. Teaching multivariable control using the quadruple-tank process. *Decision and Control, 1999. Proceedings of the 38th IEEE Conference on*, 1:807 –812 vol.1, 1999.

[38] Håkan Hjalmarsson. System identification of complex and structured systems. In *European Control Conference*, pages 3424–3452, Budapest, Hungary, August 2009.

[39] X. Bombois, G. Scorletti, M. Gevers, P.M.J. Van den Hof, and R. Hildebrand. Least costly identification experiment for control. *Automatica*, 42(10):1651 – 1662, 2006.

[40] G. C. Calafiore and M. C. Campi. The scenario approach to robust control design. *IEEE Transactions on Automatic Control*, 51(5):742–753, 2006.

[41] T. Alamo, R. Tempo, and E. F. Camacho. Improved sample size bounds for probabilistic robust control design: A packet-based strategy. In *Proceedings of the 46th IEEE Conference on Decision and Control (CDC)*, pages 6178–7183, 2007.

[42] T. Alamo, R. Tempo, and E. F. Camacho. Statistical learning theory: A packet-based strategy for uncertain feasibility and optimization problems. In V. D. Blondel, S. P. Boyd, and H. Kimura, editors, *Recent Advances in Learning and Control*. Springer-Verlag, London, 2008.

[43] M. C. Campi and S. Garatti. The exact feasibility of randomized solutions of uncertain convex programs. *SIAM Journal on Optimization (to appear)*, 2007. Available at Optimization Online, http://www.optimization-online.org/.

[44] D. Barcelli and A. Bemporad. Decentralized model predictive control of dynamically-coupled linear systems: Tracking under packet loss. In *1st IFAC Workshop on Estimation and Control of Networked Systems*, pages 204–209, Venice, Italy, 2009.